

# Re-opening dark matter windows compatible with a diphoton excess

Giorgio Arcadi<sup>a</sup> Pradipta Ghosh,<sup>a,b</sup> Yann Mambrini<sup>a</sup> and Mathias Pierre<sup>a</sup>

<sup>a</sup>Laboratoire de Physique Théorique, CNRS, Univ. Paris-Sud, Université Paris-Saclay, 91405 Orsay, France

<sup>b</sup>Centre de Physique Théorique, Ecole polytechnique, CNRS, Université Paris-Saclay, 91128 Palaiseau Cedex, France

E-mail: [giorgio.arcadi@th.u-psud.fr](mailto:giorgio.arcadi@th.u-psud.fr), [pradipta.ghosh@th.u-psud.fr](mailto:pradipta.ghosh@th.u-psud.fr), [yann.mambrini@th.u-psud.fr](mailto:yann.mambrini@th.u-psud.fr), [mathias.pierre@th.u-psud.fr](mailto:mathias.pierre@th.u-psud.fr)

**Abstract.** We investigate a simple setup in which an excess in the di-photon invariant mass distribution around 750 GeV, as seen by the ATLAS and CMS collaborations, is originated through a pair of collimated photon pairs. In this framework a scalar state  $s$  decays into two light pseudo-Goldstone bosons  $a$ , each of which subsequently decays into a pair of collimated photons which are misidentified as a single photon. In a minimal context of spontaneous symmetry breaking, we show that coupling a complex scalar field  $\Phi = (s + ia)/\sqrt{2}$  to a fermionic dark matter candidate  $\chi$ , also responsible for generating its mass, allows for the correct relic density in a large region of the parameter space, while not being excluded by the direct or indirect detection experiments. Moreover, the correct relic abundance can naturally co-exist with a relatively large width for the resonant field  $s$ .

**Keywords:** dark matter theory, particle physics - cosmology connection

**ArXiv ePrint:** [1603.05601](https://arxiv.org/abs/1603.05601)

---

## Contents

<b>1</b>	<b>Introduction</b>	<b>1</b>
<b>2</b>	<b>The Model</b>	<b>3</b>
<b>3</b>	<b>The LHC analysis</b>	<b>5</b>
3.1	Condition to mimic a di-photon process	5
3.2	Di-jet constraint	7
3.3	Fitting the di-photon excess	8
<b>4</b>	<b>The analysis implementing the dark sector</b>	<b>9</b>
4.1	$m_\chi \lesssim 375$ GeV	9
4.2	$m_\chi > 375$ GeV	11
4.3	Very light case : the freeze in regime	12
4.4	Dark Matter Detection	14
4.5	Summary	16
<b>5</b>	<b>Conclusion</b>	<b>18</b>

---

## 1 Introduction

Recently the ATLAS [1] and CMS [2] collaborations have reported an excess in the di-photon invariant mass distribution in the vicinity of 750 GeV in their 13 TeV data at the level of  $10 \pm 3$  fb [1] and  $6 \pm 3$  fb [2], respectively which can be interpreted as a (pseudo)scalar resonance with a (relatively) large width. The ATLAS has analyzed  $3.2 \text{ fb}^{-1}$  of data and observed a local significance of  $3.9\sigma$  for an excess peaked at 750 GeV whereas the CMS, using  $3.3 \text{ fb}^{-1}$  of data, has reported a local significance of  $2.8\sigma - 2.9\sigma$  [3] for an excess peaked at<sup>1</sup> 760 GeV. The global significance is reduced to  $2.0\sigma$  [4] and  $< 1\sigma$  [3] for the ATLAS and CMS, respectively. These announcements have initiated a large amount of works on the subject [5–160], trying to fit the data in effective frameworks [161–168], featuring loop induced (typically by new vector-like fermions, with respect to the standard model (SM)) couplings of the resonance, say  $s$  for example, with gluons and photons which are described by dimension five operators of the form:

$$-\mathcal{L}_0 = \frac{c_{BB}}{\Lambda} s B^{\mu\nu} B_{\mu\nu} + \frac{c_{WW}}{\Lambda} s W_i^{\mu\nu} W_{\mu\nu}^i + \frac{c_{GG}}{\Lambda} s G_\alpha^{\mu\nu} G_{\mu\nu}^\alpha, \quad (1.1)$$

where  $B_{\mu\nu}$ ,  $W_{\mu\nu}^i$  and  $G_{\mu\nu}^\alpha$  are the  $U(1)_Y$ ,  $SU(2)_L$  and  $SU(3)_C$  field strength, respectively. The parameter  $\Lambda$  represents the scale at which new dynamics appears, which is typically of the order of the mass of new fermions entering in the loop to generate an effective Lagrangian as shown in eq. (1.1). However, it was quickly realized that, in the presence of couplings only with gluons and photons, in order to produce the observed production cross-section  $\sim \mathcal{O}(10 \text{ fb})$  and simultaneously a rather large decay width of the resonance,  $\Gamma_s$ , such that  $\Gamma_s/m_s \sim 1 - 10\%$  [3, 4] with  $m_s$  giving the mass of the resonance, large values of the coupling  $c_{GG}$  would be essential. This possibility, however, contradicts (see ref. [169]) with the current

---

<sup>1</sup> Combining with  $19.7 \text{ fb}^{-1}$  of data at 8 TeV, the largest CMS excess, assuming a narrow width, i.e.,  $\sim \mathcal{O}(0.1 \text{ GeV})$ , appears at 750 GeV with a local and global significance of  $3.4\sigma$  and  $1.6\sigma$ , respectively [3].

observations from di-jet searches  $gg \rightarrow s \rightarrow gg$  at the LHC [170, 171], predicting  $c_{GG} \lesssim 0.1$  for  $\Lambda \sim 2$  TeV. Similarly, high values,  $\gtrsim 0.1$ , of the coupling  $c_{BB}$  are disfavoured<sup>2</sup>, given the constraint from the production through photon fusion [172].

A possible solution to increase  $\Gamma_s$  can be achieved by allowing new decay channels for the resonance. An intriguing possibility is represented by the case in which the additional width is provided by the decay channel into dark matter pairs. Along this line, the authors of refs. [47, 173–175] (see also ref. [176]) have considered a coupling of the resonance with a fermionic (Dirac or Majorana) dark matter candidate as:

$$-\mathcal{L}_1 = g_\chi s \bar{\chi} \chi + m_\chi \bar{\chi} \chi, \quad (1.2)$$

with  $g_\chi$  as the relevant Yukawa coupling and  $m_\chi$  representing the mass of the dark matter  $\chi$ .

However, all these studies converged to show that in the said scenario, the direct detection (in the case of a scalar resonance) or the indirect detection (in the case of a pseudoscalar resonance), strongly constraints the dark matter mass up to  $\sim \mathcal{O}(1$  TeV), due to the concerned values of  $c_{GG}$  and  $c_{BB}$  couplings, respectively. These associated values, even after respecting the di-jet [169] and photon fusion [172] constraints, appear naturally to accommodate the observed di-photon production cross-section. Combining these limits further with the constraints from monojet searches [177, 178],  $gg \rightarrow \bar{\chi} \chi g$ , the light dark matter region,  $m_\chi \lesssim 375$  GeV, i.e.,  $m_\chi \lesssim m_s/2$  appears excluded [175].

An interesting alternative has been proposed in refs. [179–182], considering the possibility that the di-photon production process  $pp \rightarrow s \rightarrow \gamma\gamma$  can be mimicked by a process of the form  $pp \rightarrow s \rightarrow aa \rightarrow 4\gamma$ , where  $a$  is a light pseudoscalar decaying into two collimated photons. In this scenario a sizable contribution to  $\Gamma_s$  could come from the  $s \rightarrow aa$  decay process. This possibility has been investigated, for instance, in ref. [182], where the  $saa$  coupling is generated by the spontaneous breaking of a Peccei-Quinn (PQ) symmetry. However, a sizable  $saa$  coupling to secure  $\Gamma_s = 40$  GeV through  $s \rightarrow aa$  decay process is rather unnatural since it would require a small PQ scale  $\sim \mathcal{O}(300$  GeV). Thus, the presence of an invisible branching fraction ( $Br$ ) has nevertheless been invoked, although the new final states have not been identified as dark matter candidates. The similar and extensive studies have been performed in the case of the next-to-minimal supersymmetric standard model (NMSSM) [183–185]. In this model the LHC signal can be reproduced only for masses  $\sim \mathcal{O}(100$  MeV) of the lightest CP-odd Higgs<sup>3</sup> since otherwise its branching ratio into two photons would be heavily suppressed compared to the same into SM fermion pairs.

In this work, we will combine the two preceding approaches in the context of a simple model featuring spontaneously broken symmetry. The coupling  $saa$  is induced after the spontaneous symmetry breaking by a classical potential term  $|\Phi|^4 \rightarrow |(s + ia)|^4$ . Thus, the derived  $saa$  coupling remains proportional to the quartic coupling. The same complex scalar field  $\Phi$  is also coupled to the dark matter  $\chi$  and, is responsible for generating  $m_\chi$  after the spontaneous symmetry breaking.

We will show that when  $\Gamma_s$  is primarily determined by  $s \rightarrow aa$  process, i.e., via  $\Gamma(s \rightarrow aa)$ , the di-photon excess can be obtained for values of  $c_{GG}$  well below 0.1, the limit predicted from the di-jet constraint. Such low values of  $c_{GG}$  couplings, as an outgrowth, strongly relax the constraints from monojet and direct dark matter searches while still remain compatible with the WMAP/PLANCK [188, 189] favoured values of the dark matter relic density.

<sup>2</sup>This scenario corresponds to  $c_{WW} = 0$  in eq. (1.1).

<sup>3</sup>Collimated photons from a light CP-odd Higgs in the NMSSM were previously studied in refs. [186, 187].

Regarding the WMAP/PLANCK constraints, three regions of the parameters space are now open: (i) the electroweak-scale dark matter ( $m_\chi \simeq 100$  GeV), (ii) a heavier window ( $\gtrsim 400$  GeV, i.e.,  $\gtrsim m_s/2$ ) and (iii) a very light case (keV dark matter). For all of these windows, we have checked that the direct and indirect detection limits are respected and are compatible with a relatively large width of the scalar, exchanged as a mediator. Our results are summarized in the final plot where we have shown points respecting all the relevant LHC constraints (e.g., di-jet, monojet, etc.), observations (di-photon production cross-section and large  $\Gamma_s$ ) and giving, at the same time, the correct relic abundance for the dark matter.

The paper is organized as follows. After a summary of the model in section 2, we will briefly review under which conditions the process  $pp \rightarrow s \rightarrow aa \rightarrow 4\gamma$  can mimic the observed di-photon signal. We will then determine the parameter space allowed by the LHC observations, and show that the di-photon signal can remain compatible with a large width of  $s$  in section 3. In the next section we introduce the dark matter candidate and compute its relic abundance, evaluating the parameter space respecting at the same time the observed di-photon excess and the WMAP/PLANCK constraints. Finally we conclude.

## 2 The Model

The Lagrangian of eq. (1.1) can be expressed for a complex scalar  $\Phi$  in a similar way. Adding a SM singlet fermion (Majorana or Dirac like) further with eq. (1.1) is straightforward. The complete Lagrangian can then be written as:

$$\mathcal{L} = \mathcal{L}_0 + \mathcal{L}_\Phi + \mathcal{L}_\chi, \quad (2.1)$$

with

$$\begin{aligned} -\mathcal{L}_0 &= \frac{c_{BB}}{\Lambda} \Phi B^{\mu\nu} B_{\mu\nu} + \frac{c_{WW}}{\Lambda} \Phi W_i^{\mu\nu} W_{\mu\nu}^i + \frac{c_{GG}}{\Lambda} \Phi G_\alpha^{\mu\nu} G_{\mu\nu}^\alpha \\ &\quad - \frac{ic_{BB}}{\Lambda} \Phi B^{\mu\nu} \tilde{B}_{\mu\nu} - \frac{ic_{WW}}{\Lambda} \Phi W_i^{\mu\nu} \tilde{W}_{\mu\nu}^i - \frac{ic_{GG}}{\Lambda} \Phi G_\alpha^{\mu\nu} \tilde{G}_{\mu\nu}^\alpha + \text{h.c.}, \end{aligned} \quad (2.2)$$

where  $\tilde{B}_{\mu\nu}$ ,  $\tilde{W}_{\mu\nu}^i$ ,  $\tilde{G}_{\mu\nu}^\alpha$  denote the dual field strength, e.g.  $\tilde{B}_{\mu\nu} = \frac{1}{2}\epsilon_{\mu\nu\rho\sigma}B^{\rho\sigma}$ , and  $\Phi = (s + ia)/\sqrt{2}$  is a complex scalar field whose Lagrangian can be expressed as:

$$\mathcal{L}_\Phi = \partial_\mu \Phi \partial^\mu \Phi^* + \mu_\Phi^2 |\Phi|^2 - \lambda_\Phi |\Phi|^4 + \frac{\epsilon_\Phi^2}{2} (\Phi^2 + \text{h.c.}). \quad (2.3)$$

We can see that eq. (2.3) contains a term that explicitly breaks the  $U(1)$  symmetry, giving mass to the Goldstone boson  $a$ , which is then promoted to a pseudo-Goldstone state. A dark matter  $\chi$  can naturally be introduced in this framework through the Lagrangian<sup>4</sup>:

$$\begin{aligned} \mathcal{L}_\chi &= \frac{1}{2} i \bar{\chi} \gamma^\mu \partial_\mu \chi - g_\chi \Phi \bar{\chi} \chi + \text{h.c.} \\ &= \frac{1}{2} i \bar{\chi} \gamma^\mu \partial_\mu \chi - \frac{g_\chi}{\sqrt{2}} s \bar{\chi} \chi - i \frac{g_\chi}{\sqrt{2}} a \bar{\chi} \gamma^5 \chi. \end{aligned} \quad (2.4)$$

Once  $\Phi$  acquires a vacuum expectation value ( $vev$ ) through the spontaneous symmetry breaking mechanism,  $\Phi = \frac{1}{\sqrt{2}}(v_\Phi + s + ia)$  with  $v_\Phi^2 = \frac{\mu_\Phi^2}{\lambda_\Phi} + \frac{\epsilon_\Phi^2}{\lambda_\Phi} \simeq \frac{\mu_\Phi^2}{\lambda_\Phi}$ , it generates automatically

<sup>4</sup>We will work in the framework of Majorana dark matter throughout this analysis. The extension to the Dirac case is straightforward.

the mass of  $s$  ( $m_s = \sqrt{2\lambda_\Phi v_\Phi}$ ), the  $saa$  coupling ( $\lambda_{saa} = \lambda_\Phi v_\Phi$ ) and the dark matter mass ( $m_\chi = \sqrt{2}g_\chi v_\Phi$ ). Moreover, the parameter  $\Lambda$  in eq. (2.2) can always be freely chosen up to a redefinition of the couplings  $c_{ii}$ 's. Choosing logically  $\Lambda = v_\Phi$ , being the scale of new physics, one can eliminate  $v_\Phi$  and re-express the relevant part of the Lagrangian (see eq. (2.2)) as the function of masses and couplings as:

$$\begin{aligned}
-\mathcal{L} \supset & \frac{\sqrt{\lambda_\Phi} C_{GG}}{m_s} s G_{\mu\nu}^\alpha G^{\mu\nu}_\alpha + \frac{\sqrt{\lambda_\Phi} C_{GG}}{m_s} a G_{\mu\nu}^\alpha \tilde{G}^{\mu\nu}_\alpha \\
& + \frac{\sqrt{\lambda_\Phi} C_{BB} c_W^2}{m_s} s F_{\mu\nu} F^{\mu\nu} + \frac{\sqrt{\lambda_\Phi} C_{BB} c_W^2}{m_s} a F_{\mu\nu} \tilde{F}^{\mu\nu} \\
& + \frac{m_s^2}{2} s^2 + \frac{m_a^2}{2} a^2 + \sqrt{\frac{\lambda_\Phi}{2}} m_s s a^2 + \sqrt{\frac{\lambda_\Phi}{2}} m_s s^3 + \frac{\lambda_\Phi}{4} (s^2 + a^2)^2 \\
& + \frac{1}{2} m_\chi \bar{\chi} \chi + \sqrt{\frac{\lambda_\Phi}{2}} \frac{m_\chi}{m_s} (s \bar{\chi} \chi + i a \bar{\chi} \gamma^5 \chi),
\end{aligned} \tag{2.5}$$

where  $C_{ii} = 2c_{ii}$ ,  $c_W^2 = \cos^2 \theta_W$ ,  $F_{\mu\nu}(\tilde{F}_{\mu\nu})$  is the field(dual field) strength for the photon field,  $m_a = \sqrt{2}\epsilon_\Phi$  is the pseudoscalar mass and we have worked with<sup>5</sup>  $c_{WW} \rightarrow 0$ . If now one fixes the mass of the scalar at 750 GeV, all the physics is then completely determined by a set of five parameters ( $C_{GG}$ ,  $C_{BB}$ ,  $\lambda_\Phi$ ,  $m_a$ ,  $m_\chi$ ). If one further wants to fit simultaneously, the width of  $s$ , the di-photon cross-section and the relic abundance, one is left with only two free parameters. The model then becomes very predictive.

Notice that, sticking to an effective field theory approach, the dimension-5 interaction terms in eq. (2.2), between the field  $\Phi$  and the SM gauge bosons, do not preserve the  $U(1)$  symmetry. As already mentioned, an explicit breaking of the  $U(1)$  symmetry has already been introduced in eq. (2.3) in order to have a non-zero mass for the pseudoscalar field  $a$  and thus, the presence of these dimension-5 operators is rather natural. Moreover, in the studied scenario, as will be clarified subsequently, the coefficients of these operators, e.g.,  $C_{BB}$ ,  $C_{GG}$ , required to be much suppressed in order to generate an experimentally viable production cross-section with collimated photons. In this setup, one might also consider the inclusion of dimension-6 operators, e.g.,  $\frac{\tilde{c}_{GG}}{\Lambda^2} \Phi^\dagger \Phi G_a^{\mu\nu} G_{\mu\nu}^a$ , which preserve the  $U(1)$  symmetry. These terms, with the choice of  $\Lambda = v_\Phi$ , after spontaneous breaking of the  $U(1)$  symmetry would produce new effective dimension-5 interactions for the scalar, featuring the same  $1/v_\Phi$  suppression associated with the  $U(1)$  violating ones. This would modify the trilinear couplings between the scalar component of  $\Phi$  and the SM gauge bosons and thus, will affect the production vertex and decay width of the scalar field. Now, as will be explained later, in the studied framework the decay width is dominated by the tree-level  $saa$  coupling and hence, the impact of including dimension-6 terms would hardly affect our findings. The relevant interactions for the pseudoscalar, however, remain the same since only dimension-5 operators can lead to couplings linear in the  $a$  field.

The main purpose of this paper is to provide a phenomenological explanation of the di-photon excess through the production of collimated photon pairs simultaneously with the main aspects of dark-matter physics. For this reason in our analysis we will freely vary the couplings of various operators and hence, the effect of dimension-6 operators can be straightforwardly encapsulated through a redefinition, including the contributions from different di-

---

<sup>5</sup>The coupling  $C_{BB}$ , from the requirement of gauge invariance, also generates interactions like  $sZZ$ ,  $sZ\gamma$ , etc. We, however, do not explore them in detail since they are observed to have a marginal impact in our analysis.

mensionalities, of the effective couplings between the scalar field  $s$  and the SM gauge bosons. Thus, we will not explicitly refer any further to the presence of dimension-6 operators.

The existence of dimension-six interactions, nevertheless, would appear effective for the pair production of  $ss$  or  $aa$  which would lead to characteristic signals, e.g.,  $gg \rightarrow ss \rightarrow 4a \rightarrow 8\gamma$ . A detail and subsequent discussion of such signal, however, is beyond the scopes of the current article.

We note in passing that for this work we consider the width of the resonance in the span of 4 – 60 GeV, the di-photon production cross-section in the range of 1 – 10 fb and finally, the relic density  $\Omega h^2 \approx 0.12$  [189].

### 3 The LHC analysis

#### 3.1 Condition to mimic a di-photon process

The decay of a substantially light pseudoscalar can produce highly collimated photons (dubbed as “photon jets”) which can be potentially misidentified as a single photon. The minimal condition to realize this kind of scenario is that the opening angle  $\Delta\phi \sim 2/\gamma$  ( $\gamma = m_s/2m_a$ , being the boost factor) of the two photons emitted in the  $a \rightarrow \gamma\gamma$  process remains below the angular resolution of the LHC detectors, which is  $\sim \mathcal{O}(20 \text{ mrad})^6$  [190, 191]. This condition provides an upper bound as  $m_a \lesssim 2 \text{ GeV}$  [179, 192, 193]. At the same time, a very high boost typically generates an enhanced decay length for  $a$ . In order to mimic the LHC di-photon signal, the decay should occur before the electromagnetic calorimeter (ECAL), which is at a distance of  $\sim 1$  meter from the collision point. A minimal requirement is then set on the decay length of  $a$ ,  $l = \beta\gamma/\Gamma_a \ll 1$  meter, where  $\beta\gamma = \sqrt{\gamma^2 - 1}$  and  $\Gamma_a$  represents the total decay width for  $a$ . This constraint is mostly relevant for values of  $m_a \lesssim 3m_{\pi^0}$  ( $m_{\pi^0}$  denotes the neutral pion mass), such that only the decay process  $a \rightarrow \gamma\gamma$  remains actually accessible<sup>7</sup>. As a consequence, the decay length, for  $m_a \lesssim 3m_{\pi^0}$ , can be expressed only as the function of  $m_a$  and  $C_{BB}$  as:

$$l \approx 7.3 \text{ cm} \left( \frac{m_s}{750 \text{ GeV}} \right)^3 \left( \frac{500 \text{ MeV}}{m_a} \right)^4 \left( \frac{0.05}{\Gamma_s/m_s} \right) \left( \frac{0.01}{C_{BB}} \right)^2. \quad (3.1)$$

Now the requirement of  $l \lesssim 1$  meter gives the following lower bound on  $C_{BB}$ :

$$C_{BB} \gtrsim 2.7 \times 10^{-3} \left( \frac{m_s}{750 \text{ GeV}} \right)^{3/2} \left( \frac{500 \text{ MeV}}{m_a} \right)^2 \left( \frac{0.05}{\Gamma_s/m_s} \right)^{1/2}. \quad (3.2)$$

We remark that eq. (3.2) should be regarded as a conservative bound. As argued in ref. [181], for example, displaced photons from  $a \rightarrow \gamma\gamma$  process corresponding to  $l \sim 1 - 10$  cm, might already be distinguishable from a pair of prompt photons originating from  $s \rightarrow \gamma\gamma$  process.

We present in figure. 1, for illustration, the allowed  $m_a$  values according to the one of  $C_{BB}$ , demanding a pair of collimated photons from  $a \rightarrow \gamma\gamma$  process. This plot is made with a fixed value of  $C_{GG} = 0.0005$  and of  $\lambda_\Phi$ , corresponding to  $\Gamma_s = 40 \text{ GeV}$ . A further constraint on the associated decay length  $l \lesssim 1$  meter disfavors the gray coloured region corresponding to  $m_a \lesssim 200 \text{ MeV}$ . For reference we have also plotted the line corresponding to  $l = 10 \text{ cm}$  in the  $(m_a, C_{BB})$  plane. We also show the  $m_a \lesssim 100 \text{ MeV}$  region, as reported in ref. [194],

<sup>6</sup>This corresponds to  $\sim 1.15^\circ$ .

<sup>7</sup>One should note that in this regime the invisible branching fraction from  $a \rightarrow \bar{\chi}\chi$  process remains negligible, given the suppression of the  $a\bar{\chi}\chi$  coupling (see eq. (2.5)) for  $m_\chi \lesssim m_a/2$ .

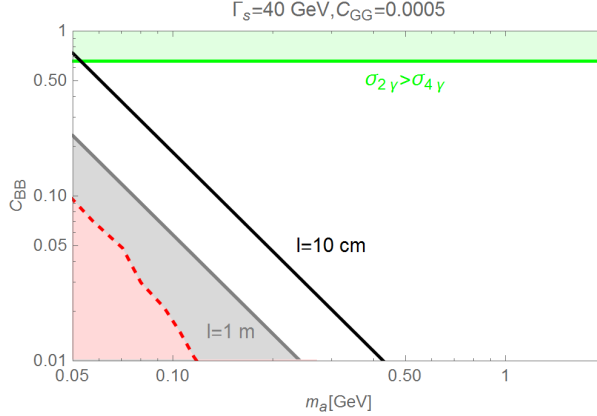


**Figure 1.** Allowed region in the  $(m_a, C_{BB})$  plane when  $a \rightarrow \gamma\gamma$  process leads to a collimated photon pairs and simultaneously, the associated decay length remains  $\lesssim 1$  meter (excluding the gray coloured region). The black coloured solid line represents a typical displaced decay with  $l = 10$  cm. The red coloured region is excluded by constraints reported in ref. [194]. The green coloured region corresponds to  $\sigma_{2\gamma} > \sigma_{4\gamma}$  which is duly explained in the text.

(represented by the red coloured region) which remains constrained from the direct searches of a light pseudoscalar in beam-dump and fixed target experiments.

It is important to note that the process  $pp \rightarrow s \rightarrow \gamma\gamma$  is also possible in our model since  $s$ , just like  $a$ , can couple to two photons through the same coupling  $C_{BB}$ . We have thus represented (in green colour) in figure 1 the region where<sup>8</sup>  $\sigma_{2\gamma} \equiv \sigma(pp \rightarrow s \rightarrow \gamma\gamma) > \sigma_{4\gamma} \equiv \sigma(pp \rightarrow s \rightarrow aa \rightarrow 4\gamma)$ .

The allowed range,  $0.2 \text{ GeV} \leq m_a \leq 2 \text{ GeV}$ , can be constrained further by considering suitable isolation cuts. Indeed, experimental searches of the somewhat similar  $h \rightarrow aa \rightarrow 4\gamma$  process, with  $h$  being the SM Higgs boson, can discriminate, through suitably defined calorimeter variables, isolated photons from the ones coming from  $\pi^0$  decays. Given the similarity between the  $\pi^0 \rightarrow \gamma\gamma$  and  $a \rightarrow \gamma\gamma$  processes, it is useful to adopt those variables to reduce the probability of faking single photon signals [200].

We have then redetermined, in figure 2 the allowed parameter space in the  $(m_a, C_{BB})$  plane, for  $C_{GG} = 0.001$  and for four values of  $\lambda_\Phi$ , ranging from 0.25 to 4 giving  $\Gamma_s$  in the span of 4 GeV to 60 GeV, by using the treatment illustrated in ref. [182]. The upper limit on  $m_a$ , compared to figure 1, is now lowered to 500 – 600 MeV (based on the similar considerations a slightly weaker limit of 800 MeV has been found in ref. [181]). Interestingly, most of the allowed parameter space now lies below the threshold of  $3m_{\pi^0}$ , above which the hadronic decays become accessible for the pseudoscalar. As a consequence, in this regime,  $Br(a \rightarrow \gamma\gamma) = 1$  irrespective of the values of  $C_{BB}$  and  $C_{GG}$ . As will be clarified in the next section, this will lead to a rather predictive scenario. To utilize this predictive behaviour, we will use this region of the parameter space for most of the analytical estimates presented in this work. In the absence of a dedicated experimental study, we have nevertheless included the region  $m_{3\pi^0} \leq m_a \leq 2 \text{ GeV}$  in the numerical computations.

We finally remark that the allowed parameter space can be constrained even further by considering the different photon conversion rate, i.e., the probability of the interaction of a

<sup>8</sup>In reality in figure 1 the region corresponding to  $C_{BB} \gtrsim 0.1$  is excluded by the 8 TeV searches of  $s \rightarrow ZZ, Z\gamma$  processes [195–199]. One should interpret figure 1 just as an illustrative plot.



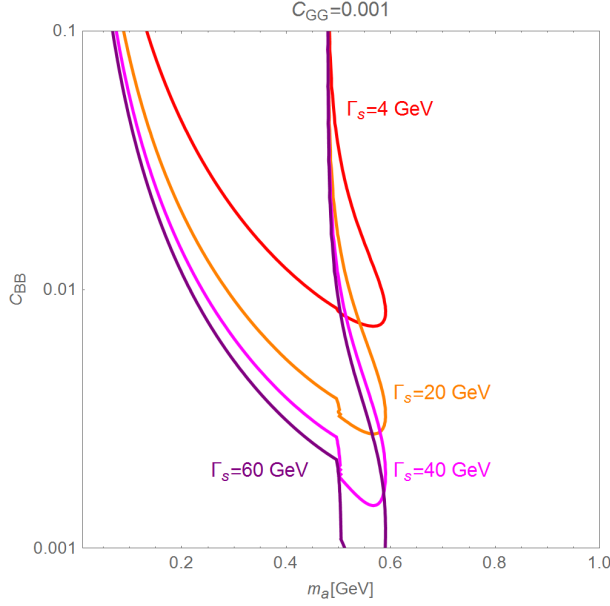


**Figure 2.** The variations of coupling  $C_{BB}$  with  $m_a$  for the different values of  $\Gamma_s$ , ensuring that the pseudoscalar decays before the ECAL and produces sufficiently collimated photon pairs to mimic the observed di-photon signal. For this plot  $C_{GG} = 0.001$ .

photon within the calorimeter to produce a  $e^+e^-$  pair, between  $2\gamma$  and  $4\gamma$  events. A detailed investigation of this possibility has been performed in ref. [179].

### 3.2 Di-jet constraint

As already emphasized, that the couplings  $C_{GG}$  and  $C_{BB}$  are constrained, by the requirement of the relative absence of additional signals, e.g., di-jets,  $Z\gamma$  or  $ZZ$  etc., compared to the di-photon one. In our scenario the strongest constraint on  $C_{GG}$  comes from the di-jet searches. For this purpose we have imposed that  $\sigma(pp \rightarrow s \rightarrow jj) < 2.5$  pb, at 8 TeV centre-of-mass<sup>9</sup> energy [170, 171].

In the  $Br(a \rightarrow \gamma\gamma) = 1$  regime the corresponding cross-section is given by:

$$\begin{aligned} \sigma(pp \rightarrow s \rightarrow jj) &= \frac{\pi^2}{8m_s \mathbf{s}} I_{GG,8TeV} \frac{2C_{GG}^2 \lambda_\Phi m_s}{\pi} Br(s \rightarrow gg) \\ &\approx \frac{\pi^2}{8m_s \mathbf{s}} I_{GG,8TeV} \frac{2C_{GG}^2 \lambda_\Phi m_s}{\pi} \frac{32C_{GG}^2}{1 + 32C_{GG}^2}, \end{aligned} \quad (3.3)$$

where we have used eq. (2.5) and retained the dependence only on the  $aa$  and  $gg$  channels (see next section) in the determination of  $\Gamma_s$ . The quantities  $\mathbf{s}$  and  $I_{GG,8TeV}$  represent the square of the centre-of-mass energy and the integral of a function involving dimensionless quantities like parton distribution functions (PDFs), evaluated at  $\sqrt{\mathbf{s}} = 8$  TeV, respectively. It can be easily seen from eq. (3.3) that the condition  $\sigma(pp \rightarrow s \rightarrow jj) < 2.5$  pb, with<sup>10</sup>  $I_{GG,8TeV} = 280$ , is satisfied for  $C_{GG} \lesssim 0.1$ .

<sup>9</sup>One can, for example, see ref. [201, 202] for a similar bound with 13 TeV centre-of-mass energy.

<sup>10</sup>Here we have considered MSTW 2008 NLO PDF [203–205] and included the next-to-leading order scaling factor.



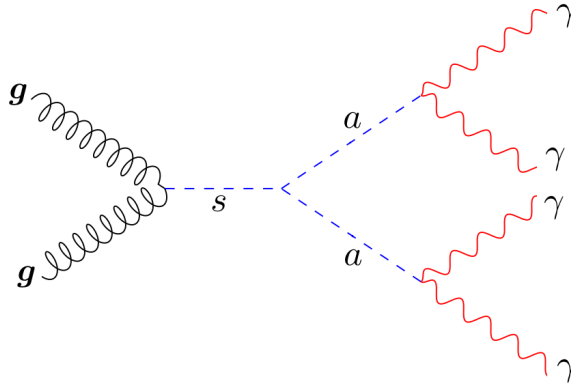


**Figure 3.** Main channel contributing to the di-photon excess observed at the LHC.

### 3.3 Fitting the di-photon excess

The production cross-section for the studied di-photon signal through the gluon fusion process  $gg \rightarrow s \rightarrow aa \rightarrow 4\gamma$  (see figure 3) is given by

$$\sigma_{4\gamma} = \frac{\pi^2}{8m_s \mathbf{s}} \Gamma(s \rightarrow gg) Br(s \rightarrow aa) [Br(a \rightarrow \gamma\gamma)]^2 I_{GG}, \quad (3.4)$$

with  $I_{GG}$  being the integral over the PDFs. This is estimated to be  $\simeq 3400$  using MSTW 2008 NLO PDF [203–205] and including the next-to-leading order scaling factor in the definition of  $I_{GG}$ . The desired signal, as already mentioned, can also be induced through the photon fusion [206] process  $\gamma\gamma \rightarrow s \rightarrow aa \rightarrow 4\gamma$ . We, however, do not consider this possibility in this article.

At this point one can use eq. (2.5) to compute:

$$\Gamma(s \rightarrow aa) = \frac{\lambda_\Phi m_s}{16\pi}, \quad \Gamma(s \rightarrow gg) = \frac{2\lambda_\Phi m_s}{\pi} C_{GG}^2. \quad (3.5)$$

Now the processes  $s \rightarrow \gamma\gamma$ ,  $s \rightarrow ZZ$ ,  $s \rightarrow Z\gamma$  are suppressed compared to  $s \rightarrow gg$  mode by factors like  $8/\cos^4 \theta_W$ ,  $8/\sin^4 \theta_W$ ,  $8/\sin^2 \theta_{2W}$ , respectively, even when  $C_{BB} \sim C_{GG}$ . The upper limit of  $C_{BB}$  is constrained from the photon fusion process. The invisible decay mode  $s \rightarrow \bar{\chi}\chi$  also suffers suppression, either from the  $s\bar{\chi}\chi$  coupling  $\propto m_\chi/m_s$  (for  $m_\chi \ll m_s$ ) or from the phase space factor (when  $m_\chi \sim m_s/2$ ). Thus, collectively one can use eq. (3.5) to get

$$Br(s \rightarrow aa) \approx \frac{1}{1 + 32C_{GG}^2}. \quad (3.6)$$

This equation is especially valid for  $m_a \lesssim 500$  MeV, i.e., below the  $3m_{\pi^0}$  threshold when  $Br(a \rightarrow \gamma\gamma) = 1$ . In this region, combining eq. (3.6) with eq. (3.4) one obtains:

$$\sigma_{4\gamma} \approx \frac{4\pi^2}{\mathbf{s}} I_{GG} \frac{C_{GG}^2}{(1 + 32C_{GG}^2)^2} \frac{\Gamma_s}{m_s} \simeq 16 \text{ fb} \frac{(\Gamma_s/m_s)}{0.05} \frac{\left(\frac{C_{GG}}{0.001}\right)^2}{(1 + 32C_{GG}^2)^2}. \quad (3.7)$$

Interestingly, for  $m_a \lesssim m_{3\pi^0}$  the  $4\gamma$  production cross-section depends only on  $C_{GG}$  and  $\lambda_\Phi$  couplings while remains independent of  $C_{BB}$ , the  $a\gamma\gamma$  coupling. Indeed, from eq. (3.7) one can see the possibility to obtain  $\sigma_{4\gamma} \sim \mathcal{O}(1 - 10 \text{ fb})$  together with a large  $\Gamma_s$  ( $\sim 5\% m_s$ ) for

low values of  $C_{GG}$ , consistent with the di-jet constraints. This comes trivially from the fact that a large  $\lambda_\Phi$  coupling is responsible for the large  $\Gamma_s$  and a sizable  $\sigma_{4\gamma}$  without requiring high values of  $C_{GG}$  and  $C_{BB}$  couplings. We finally notice that the di-jet limit,  $C_{GG} \lesssim 0.1$  implies that for all practical purposes  $\Gamma_s \approx \Gamma(s \rightarrow aa)$ . This feature allows us to trade, in the analytical expressions considered in this section, the free parameter  $\lambda_\Phi$  with the physical observable  $\Gamma_s$ .

It is important to note that although the coupling  $C_{BB}$  does not directly appear in  $\sigma_{4\gamma}$ , it is not unconstrained in nature. In fact, the absence of di-photon signal from photon fusion process and the requirement of a pseudoscalar decaying before the ECAL provide an upper and lower bound for  $C_{BB}$ , respectively. In reality, however, there exists one more way to constrain the coupling  $C_{BB}$  by demanding a suppressed  $s \rightarrow \gamma\gamma$  process. We have already used this to derive eq. (3.6). The condition  $\frac{\Gamma(s \rightarrow \gamma\gamma)}{\Gamma(s \rightarrow aa)} \ll 1$ , implies  $C_{BB} \ll 0.65$ .

A good fit for  $\sigma_{4\gamma}$  can also be obtained for  $m_a \gtrsim 500$  MeV with a sizable branching fraction of  $a$  into the hadronic channels. In such a case the cross-section is obtained by multiplying eq. (3.7) with  $(Br(a \rightarrow \gamma\gamma))^2 \approx (C_{BB}^4 c_W^8 / 64 C_{GG}^4)$  and is given by:

$$\sigma_{4\gamma} \approx 5 \text{ fb} \frac{(\Gamma_s/m_s)}{0.05} \frac{1}{(1 + 32C_{GG}^2)^2} \left(\frac{C_{BB}}{0.005}\right)^4 \left(\frac{0.005}{C_{GG}}\right)^2. \quad (3.8)$$

The condition for the dominance of  $s \rightarrow 4\gamma$  channel compared to  $s \rightarrow \gamma\gamma$  mode is similarly modified and becomes:

$$C_{GG} \lesssim 0.27 C_{BB}^{1/2}. \quad (3.9)$$

## 4 The analysis implementing the dark sector

Once one couples the dark matter to the field  $\Phi$  through eq. (2.4), one can compute the relic abundance of  $\chi$  as a function of  $C_{GG}$  and  $\lambda_\Phi$  for different  $m_\chi$  values and check if there exists parameter space compatible with the observed di-photon excess. The result is presented in figure 4 where we have shown in the  $(\lambda_\phi, C_{GG})$  plane the parameter space allowed by the three constraints, namely: (i)  $1 \text{ fb} \leq \sigma_{4\gamma} \leq 10 \text{ fb}$ , (ii)  $4 \text{ GeV} \leq \Gamma_s \leq 60 \text{ GeV}$  and (iii) correct relic abundance  $\approx 0.12$  [189]. It is evident from figure 4 that for any value of the dark matter mass between 200 GeV to 700 GeV, there exist values of  $C_{GG}$  that give a  $\sigma_{4\gamma} \sim \mathcal{O}(1 - 10 \text{ fb})$  together with  $4 \text{ GeV} \lesssim \Gamma_s \lesssim 60 \text{ GeV}$  while still respecting the PLANCK constraints. We will study the different regimes in detail in the following sub-sections.

### 4.1 $m_\chi \lesssim 375 \text{ GeV}$

For  $m_a < m_\chi \lesssim m_s/2$  the dark matter can annihilate into  $\gamma\gamma$ ,  $gg$  and  $aa$ , as well as into  $Z\gamma$  and  $ZZ$ , whether kinematically open (the last two modes are suppressed in the setup considered in this work).

The  $\gamma\gamma$  and  $gg$  channels mostly originate from s-channel exchange of the pseudoscalar. The corresponding thermally averaged cross-sections, using eq. (3.6) and eq. (3.7), can be

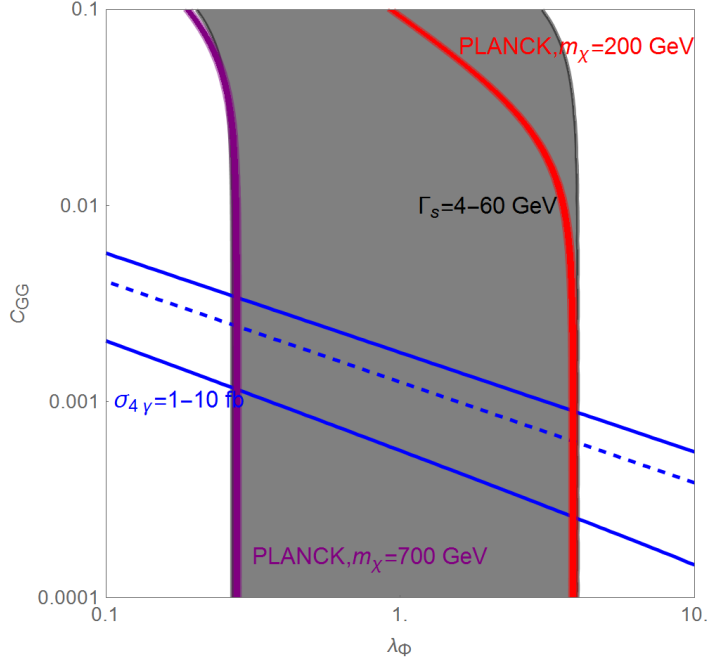


**Figure 4.** The allowed parameter space in the  $(\lambda_\Phi, C_{GG})$  plane consistent with the observations of: (a) correct relic density, (b) the observed di-photon production cross-section and (c) a relatively large width of the resonance. The gray coloured band corresponds to the large width region (4 – 60 GeV) whereas the blue coloured lines (solid and dashed) represent a di-photon production cross-section of 1 – 10 fb, as observed at the LHC. The red and magenta coloured lines correspond to points that respect the PLANCK constraints for  $m_\chi = 200$  GeV and 700 GeV, respectively. For this plot we consider  $C_{BB} = 0.005$ .

estimated as [47, 173, 174]:

$$\begin{aligned}
\langle\sigma v\rangle_{gg} &= \frac{16\lambda_\Phi^2 C_{GG}^2 m_\chi^2}{\pi m_s^4} \approx 5 \times 10^{-30} \left(\frac{\sigma_{4\gamma}}{16 \text{ fb}}\right) \left(\frac{\Gamma_s/m_s}{0.05}\right) \left(\frac{m_\chi}{100 \text{ GeV}}\right)^2 \left(\frac{750 \text{ GeV}}{m_s}\right)^4, \\
\langle\sigma v\rangle_{\gamma\gamma} &= \frac{2\lambda_\Phi^2 C_{BB}^2 C_W^4 m_\chi^2}{\pi m_s^4} \\
&\approx \frac{9 \times 10^{-27}}{(1 + 32C_{GG}^2)^2} \left(\frac{C_{BB}}{0.1}\right)^2 \left(\frac{\Gamma_s/m_s}{0.05}\right)^2 \left(\frac{m_\chi}{100 \text{ GeV}}\right)^2 \left(\frac{750 \text{ GeV}}{m_s}\right)^4, \quad (4.1)
\end{aligned}$$

in the unit of  $\text{cm}^3\text{s}^{-1}$ . We now clearly see the difficulty to achieve the correct relic abundance through the s-wave channel due to the constraints on  $\sigma_{4\gamma}$  and  $C_{BB} \lesssim 0.1$  for the  $gg$  and  $\gamma\gamma$  final states, respectively. Moreover, the gluon channel is also constrained by the di-jet constraint, eq. (3.3), and, to a lesser extent and only for  $m_a \geq 500$  MeV, by the FERMI searches of gamma-rays from DSph [207, 208]. On the other hand, the contribution from the photon channel is, instead, substantially excluded by the FERMI searches of monochromatic gamma-ray signals [209], which give a limit as strong as  $10^{-(29\div 30)} \text{cm}^3\text{s}^{-1}$  for  $m_\chi \lesssim 100$  GeV.

Even if the  $aa$  channel gives rise to a p-wave velocity suppressed cross-section (by CP arguments), it is the dominant annihilation process at the decoupling time. It proceeds mostly through the  $s$ -channel exchange of the scalar  $s$  as depicted in the figure 5. The concerned

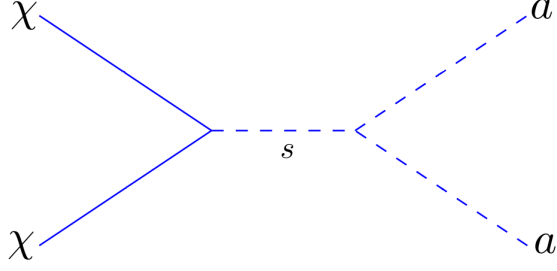


**Figure 5.** Main channel contributing to the relic abundance for  $m_\chi \lesssim 375$  GeV.

thermally averaged cross-section can be estimated as:

$$\begin{aligned}
 \langle \sigma v \rangle_{aa} &= \frac{9m_\chi^2 \lambda_\Phi^2}{384\pi m_s^4} v^2 \\
 &\approx 5.3 \times 10^{-27} \text{ cm}^3 \text{ s}^{-1} \frac{1}{(1 + 32C_{GG}^2)^2} \left( \frac{\Gamma_s/m_s}{0.05} \right)^2 \left( \frac{m_\chi}{100 \text{ GeV}} \right)^2 \left( \frac{750 \text{ GeV}}{m_s} \right)^4. \quad (4.2)
 \end{aligned}$$

In figure 6 we show the result of complete numerical analysis, performed precisely by determining the dark matter annihilation cross-sections and its relic density through the package MicrOMEGAS [210]. Fixed values for the  $C_{GG}$  and  $C_{BB}$  couplings, as 0.001 and 0.005, respectively, are used for this figure. Here we have plotted the contour of correct relic density in the  $(m_\chi, \Gamma_s)$  plane corresponding to different di-photon production cross-sections. We have also used the same methods and tools for figure 4. We notice from figure 6 that, when  $m_\chi \lesssim 375$  GeV, the correct relic density can be achieved, through the annihilation channel of figure 5, for  $m_\chi \sim \mathcal{O}(200 - 300 \text{ GeV})$  and for  $12 \text{ GeV} \leq \Gamma_s \leq 50 \text{ GeV}$  while still fitting the LHC di-photon data. We also notice the typical pole effect, i.e., when  $m_\chi$  approaches  $m_s/2$ , the width needs to be narrow to avoid the under-abundance due to thermal broadening effect [211]. On the other hand, being velocity suppressed, this channel cannot account for any indirect detection signal as it will be discussed in sub-section 4.4.

#### 4.2 $m_\chi > 375$ GeV

When  $m_\chi > m_s/2$ , the annihilation process  $\chi\chi \rightarrow sa$ , shown in figure 7, becomes kinematically allowed. This channel will dominate the annihilation process compared to  $aa$  (or  $ss$  when  $m_\chi > m_s$ ) as it is the only channel which is not velocity suppressed. The relevant thermally averaged cross-section is given by:

$$\langle \sigma v \rangle_{sa} \simeq \frac{\lambda_\Phi^2 m_\chi^2}{8\pi m_s^4} \simeq \frac{3 \times 10^{-25} \text{ cm}^3 \text{ s}^{-1}}{(1 + 32C_{GG}^2)^2} \left( \frac{\Gamma_s/m_s}{0.05} \right)^2 \left( \frac{m_\chi}{400 \text{ GeV}} \right)^2 \left( \frac{750 \text{ GeV}}{m_s} \right)^4. \quad (4.3)$$

As evident from eq. (4.3) that in the case of  $\Gamma_s/m_s \sim 5\%$ , the cross-section exceeds the thermally favoured value and leads, consequently, to an underabundant dark matter. This is also reflected from figure 6 that the correct relic density for  $m_\chi > 375$  GeV is achieved only for  $\Gamma_s < 12$  GeV. The latter, for the chosen values of  $C_{GG}$ ,  $C_{BB}$  couplings, corresponds to a value of  $\sigma_{4\gamma}$  on the lower side.

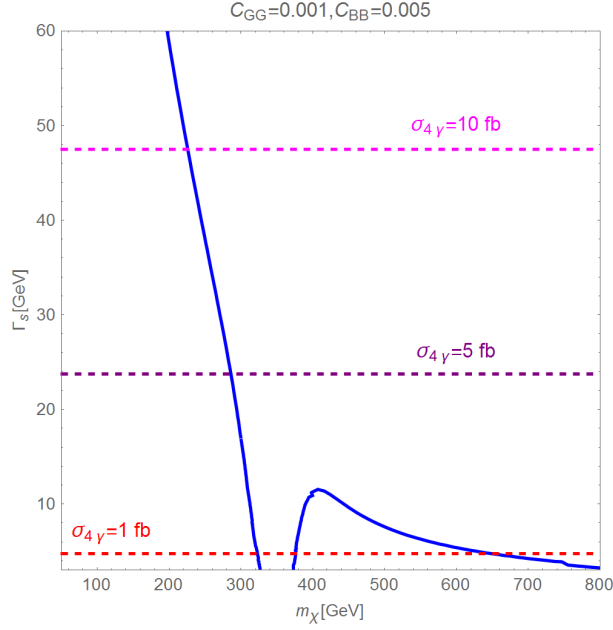


**Figure 6.** The contour of correct relic density in the  $(m_\chi, \Gamma_s)$  plane. The differently coloured horizontal lines correspond to the various values of the di-photon production cross-sections.

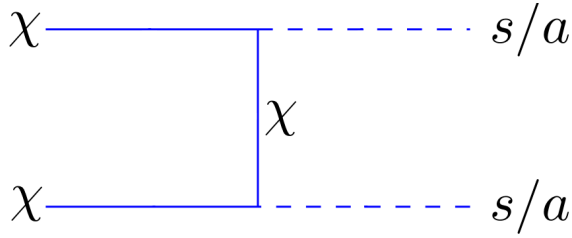


**Figure 7.** Main channel responsible for the relic abundance for  $m_\chi > 375$  GeV.

### 4.3 Very light case : the freeze in regime

In this case the dominant contribution to the dark matter relic density is given by the annihilations into  $gg$  and  $\gamma\gamma$  final states through s-channel exchange of the pseudoscalar. The corresponding thermally averaged cross-sections are:

$$\begin{aligned}
 \langle\sigma v\rangle_{gg} &= \frac{1024}{\pi} \frac{m_\chi^6}{m_a^4 m_s^4} \lambda_\Phi^2 C_{GG}^2 \\
 &\approx 3 \times 10^{-33} \text{ cm}^3 \text{ s}^{-1} \lambda_\Phi^2 C_{GG}^2 \left(\frac{m_\chi}{0.1 \text{ GeV}}\right)^6 \left(\frac{1 \text{ GeV}}{m_a}\right)^4 \left(\frac{750 \text{ GeV}}{m_s}\right)^4, \\
 \langle\sigma v\rangle_{\gamma\gamma} &= \frac{128}{\pi} \frac{m_\chi^6}{m_a^4 m_s^4} \lambda_\Phi^2 C_{BB}^2 c_W^4 \\
 &\approx 2.2 \times 10^{-34} \text{ cm}^3 \text{ s}^{-1} \lambda_\Phi^2 C_{BB}^2 \left(\frac{m_\chi}{0.1 \text{ GeV}}\right)^6 \left(\frac{1 \text{ GeV}}{m_a}\right)^4 \left(\frac{750 \text{ GeV}}{m_s}\right)^4. \quad (4.4)
 \end{aligned}$$

As evident from eq. (4.4) that these cross-sections are very far from the thermally favoured value,  $\sim \mathcal{O}(10^{-26}) \text{ cm}^3 \text{ s}^{-1}$ , such that the validity of the WIMP paradigm itself

becomes questionable. Thus, we apply the conventional rule-of-thumb of comparing the dark matter annihilation rate  $\Gamma_{\text{ann}} = \langle \sigma v \rangle n_{\chi,eq}$  with the Hubble expansion rate, both evaluated at temperature  $T \sim \mathcal{O}(m_\chi)$ . Considering for reference the  $\gamma\gamma$  annihilation channel <sup>11</sup>, one gets:

$$\frac{\Gamma_{\text{ann}}(T = m_\chi)}{H(T = m_\chi)} \approx \frac{3.2}{(1 + 32C_{GG}^2)^2} \left( \frac{\Gamma_s/m_s}{0.05} \right)^2 \left( \frac{C_{BB}}{0.005} \right)^2 \left( \frac{m_\chi}{0.1 \text{ GeV}} \right)^7 \left( \frac{0.5 \text{ GeV}}{m_a} \right)^4 \left( \frac{750 \text{ GeV}}{m_s} \right)^4. \quad (4.5)$$

For the chosen model parameters with  $m_\chi \lesssim 100$  MeV, compatible with the LHC di-photon signal, the dark matter annihilations become inefficient. The dark matter, however, still remains relativistic and the ratio  $\frac{\Gamma_{\text{ann}}}{H}$  drops very steeply as long as the dark matter mass is further reduced. The dark matter could nevertheless be kept into thermal equilibrium by the decay process  $\Gamma(a \rightarrow \bar{\chi}\chi) = \frac{\lambda_\Phi m_a m_\chi^2}{8\pi m_s^2}$ , with  $a$  in turn, kept into equilibrium by its couplings with the gauge bosons, at least down to temperatures  $\sim \mathcal{O}(m_a)$ . This requirement can be translated into the following condition:

$$\begin{aligned} \frac{\Gamma(a \rightarrow \bar{\chi}\chi)(T = m_a)}{H(T = m_a)} &\geq 1, \\ \rightarrow m_\chi &\gtrsim 1.3 \text{ keV} \sqrt{1 + 32C_{GG}^2} \sqrt{\frac{0.02}{\Gamma_s/m_s}} \left( \frac{m_a}{1 \text{ GeV}} \right)^{1/2} \left( \frac{m_s}{750 \text{ GeV}} \right). \end{aligned} \quad (4.6)$$

We thus notice that the  $a \leftrightarrow \bar{\chi}\chi$  process is rather efficient and keeps the dark matter in the equilibrium unless  $m_\chi \sim \mathcal{O}(1 \text{ keV})$  (or even below) for  $\Gamma_s/m_s > 2\%$ . Remembering that  $m_\chi$  below a keV is excluded by structure formation, we conclude that the light dark matter is coupled to the primordial thermal bath until the temperature  $T \sim m_a$ . After this temperature relativistic decoupling happens with a relic density given by:

$$\Omega_{\chi,\text{rel}} h^2 \approx 9.6 \times 10^{-2} \frac{g_{\text{eff}}}{g_{*,S}(T_d)} \left( \frac{m_\chi}{1 \text{ eV}} \right), \quad (4.7)$$

where  $g_{*,S}(T_d)$  represents the number of relativistic degrees of freedom at the temperature  $T_d$  of decoupling of the dark matter while  $g_{\text{eff}}$  is the number of internal degrees of freedom of the dark matter itself. The correct relic density can be achieved for  $m_\chi \sim 100$  eV, inconsistently with the conditions stated above. For viable values of the mass, i.e.,  $\gtrsim \mathcal{O}(\text{keV})$ , the dark matter is overabundant. For  $\Gamma_s/m_s < 2\%$ , on the contrary, there exists a small window of masses,  $m_\chi \sim 1 - 10 \text{ keV}$ , for which the dark matter cannot get into the thermal equilibrium in the Early Universe. In this case the dark matter is produced through freeze-in [212–214] by the decay of the pseudoscalar. The corresponding relic density is given by:

$$\begin{aligned} \Omega_{FI} h^2 &= \frac{1.09 \times 10^{27} g_a}{g_{*,S}(T = m_a)^{3/2}} \frac{m_\chi \Gamma(a \rightarrow \bar{\chi}\chi)}{m_a^2} \\ &\approx 0.3 \frac{1}{(1 + 32C_{GG}^2)} \left( \frac{\Gamma_s/m_s}{0.01} \right) \left( \frac{m_\chi}{1 \text{ keV}} \right)^3 \left( \frac{750 \text{ GeV}}{m_s} \right)^2 \left( \frac{1 \text{ GeV}}{m_a} \right). \end{aligned} \quad (4.8)$$

If the dark matter is not in the thermal equilibrium, the  $s \rightarrow \bar{\chi}\chi$  decay process can also give rise to freeze-in production. However, its contribution is suppressed with respect to

<sup>11</sup>As  $m_\chi$  decreases, the relevant annihilation processes occur below the temperature of the QCD phase transition,  $\sim \mathcal{O}(200 \text{ MeV})$ , and then the hadronic annihilation channel remains inaccessible.

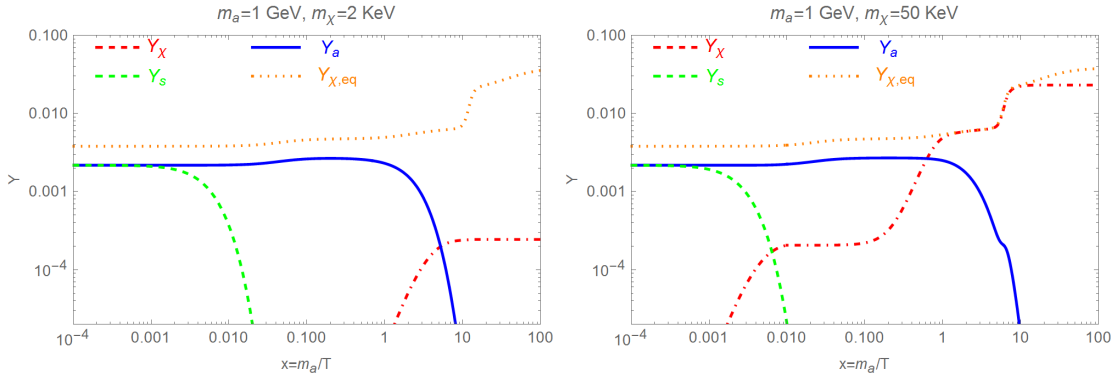


**Figure 8.** Evolution of the abundance of the  $s$ ,  $a$  and  $\chi$  fields, as determined by the numerical solution of a system of coupled Boltzmann equations in the very light dark matter regime. The two panels refer to two values of  $m_\chi$ , namely, 2 keV (left) and 50 keV (right). As evident from the comparison with the dark matter equilibrium distribution (dotted orange coloured line), that for the lighter mass, the dark matter is not capable of getting into the thermal equilibrium and it is produced through freeze-in. In the case of  $m_\chi = 50$  keV, the dark matter can however go into the thermal equilibrium and get decoupled while still being relativistic.

eq. (4.8), achieved with the replacement  $m_a \rightarrow m_s$ . As can be seen, the correct dark matter relic density requires a  $\Gamma_s$  on the smaller side, i.e.,  $\lesssim 7.5$  GeV giving  $\Gamma_s/m_s \lesssim 1\%$  or  $m_a \sim 2$  GeV.

The analytical expressions reported above have been validated by solving a system of coupled Boltzmann equations tracking the abundance of the dark matter itself as well as the ones of the scalar field  $s$  and of the pseudoscalar field  $a$ .

Two examples of the numerical solution of this system are shown in figure 8. Here two values of the dark matter masses have been considered, namely, 2 keV (left) and 50 keV (right). In the lighter dark matter case, we notice that the dark matter abundance is always well below the equilibrium one, represented by the dotted orange coloured<sup>12</sup> curve. It is produced at  $T \sim \mathcal{O}(m_a)$ , as expected for the freeze-in mechanism, and the numerical value of its abundance, as determined by the solution of the system of equations, is in very good agreement with the theoretical prediction stated in eq. (4.8). We also notice that, for the chosen set of parameters, the dark matter abundance matches the experimental expectation. On the contrary, for the heavier value of the mass, i.e., 50 keV, the dark matter abundance perfectly tracks the thermal equilibrium function until, again,  $T \sim \mathcal{O}(m_a)$  and then remains constant confirming the prediction of a relativistic decoupling. Interesting signatures of such a scenario would be the interpretation of the 3.5 keV monochromatic signal as recently observed in different clusters of galaxies [215].

#### 4.4 Dark Matter Detection

One of the main characteristics of the proposed scenario is the fact that here the observed di-photon production cross-section is obtained for relatively lower values of the  $C_{GG}$  and  $C_{BB}$  couplings, compared to the direct production from a 750 GeV resonance. As already mentioned in the introduction, such values can potentially evade the constraints from the dark matter searches. Regarding direct detection of the dark matter the most relevant interactions

<sup>12</sup>The raise of the curve at high values of  $x$  is due to the change of  $g_{*,S}$ , coming from the QCD phase transition occurring at  $T \sim \mathcal{O}(100$  MeV). The latter corresponds to  $x \sim \mathcal{O}(10)$ .



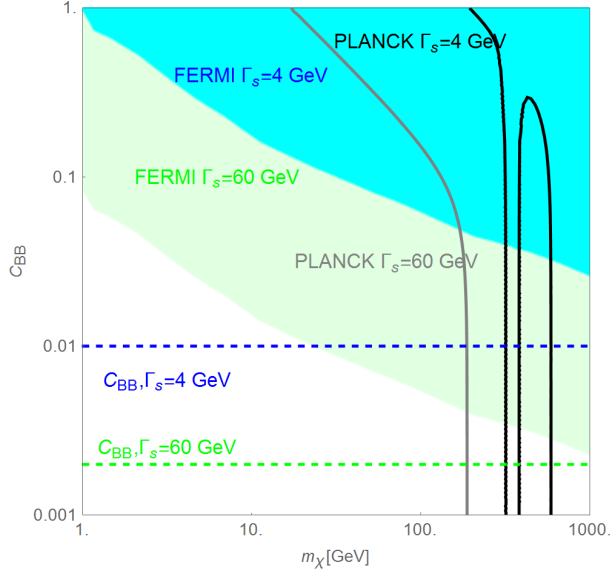


**Figure 9.** Allowed region in the  $(m_\chi, C_{BB})$  plane using the constraints from the FERMI/HESS searches of the gamma-ray lines. The cyan and light green coloured regimes, excluded from the FERMI/HESS searches, correspond to  $\Gamma_s = 4$  and  $60$  GeV, respectively. The black and gray coloured contours represent the correct relic density for the same two values of  $\Gamma_s$ . The blue and green coloured horizontal dashed lines represent two reference  $C_{BB}$  values for the same two  $\Gamma_s$  values (see figure 2), which assure a pseudoscalar decay length  $\lesssim 1$  meter for  $m_a \lesssim 500$  MeV.

are the Spin Independent (SI) ones, produced by the exchange of the scalar field  $s$ , as noted also in refs. [47, 173–175]. The SI cross-section, in the studied framework, can be written as:

$$\sigma_{\chi p}^{\text{SI}} \approx 6.7 \times 10^{-48} \text{ cm}^2 \frac{1}{(1 + 32C_{GG}^2)^2} \left( \frac{\Gamma_s/m_s}{0.05} \right)^2 \left( \frac{750 \text{ GeV}}{m_s} \right)^8 \left( \frac{m_\chi}{100 \text{ GeV}} \right)^2 \left( \frac{C_{GG}}{0.001} \right)^2, \quad (4.9)$$

which remains well below the current limit from LUX [216], given the very small value of the  $C_{GG}$  coupling. The latter also implies an very suppressed monojet production cross-section and thereby, easily evades the corresponding experimental constraint.

On the contrary, a potential impact is still retained by the indirect dark matter searches. At this moment, the most effective constraint is the one coming from the FERMI and HESS searches of the gamma-ray lines. These searches can trace  $C_{BB}$  values  $\sim \mathcal{O}(0.001)$  or even smaller. The latter, especially in the low  $m_a$  regime, may appear incompatible with the requirement of a pseudoscalar decay length  $\lesssim 1$  meter, as depicted in figure 1.

The impact of the indirect detection on the relevant model parameters is represented in figure 9. Here we have shown the excluded regions in the  $(m_\chi, C_{BB})$  plane from the FERMI/HESS searches for the minimum and maximum  $\Gamma_s$  values considered in this work, i.e.,  $4$  GeV and  $60$  GeV, respectively. The regions in the  $(m_\chi, C_{BB})$  plane excluded by the FERMI searches, corresponding to  $\Gamma_s = 4$  GeV and  $60$  GeV, are represented with the cyan and light green colour, respectively. The black and the gray coloured contours correspond to the correct relic density, as suggested by the PLANCK. It is apparent from figure 9 that one can extract a *decreasing* minimum value for  $C_{BB}$  depending on the *increasing*  $m_\chi$  value. As a reference, we also compare these limits with the ones obtained from figure 2. The latter are represented by the dashed blue coloured line (for  $\Gamma_s = 4$  GeV) and by dashed green coloured

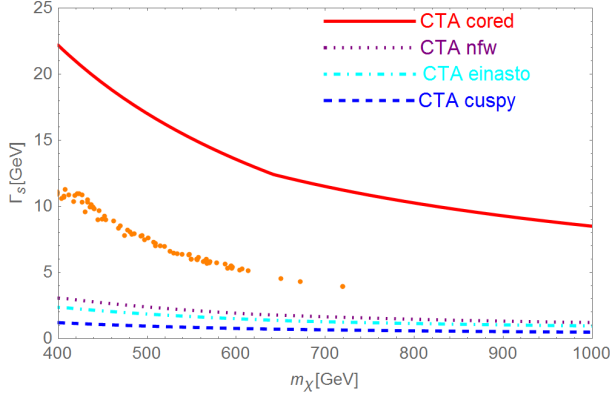


**Figure 10.** Plot showing the CTA detection prospects in the  $(m_\chi, \Gamma_s)$  plane for the gamma-ray boxes originating from the annihilation process  $\bar{\chi}\chi \rightarrow sa$ . This plot is prepared for the four possible choices of the dark matter profile, as mentioned in the plot. The orange coloured points represent the set of viable model points which emerged from the parameter scan described in the sub-section 4.4.

line (for  $\Gamma_s = 60$  GeV), respectively. One should note that the  $C_{BB}$  values considered for figure 9 always give a pseudoscalar decay length  $\lesssim 1$  meter as observed in figure 2.

Concerning detection of the dark matter, an interesting scenario appears for  $m_\chi > m_s/2$ . In this case the s-wave annihilation process  $\bar{\chi}\chi \rightarrow sa$  gives a characteristic signal represented by a wide gamma-ray box [217]<sup>13</sup> which can be probed by the CTA [218] in the near future. The detection prospects are shown in figure 10. It is evident from figure 10 that the CTA can efficiently probe the studied corner of the parameter space and thus, in the absence of any signal, can also exclude the entire viable parameter space.

#### 4.5 Summary

We summarized our results in figure 11. This plot accommodates a set of points in the  $(m_\chi, \Gamma_s)$  plane possessing the correct relic density and corresponds to different values of the diphoton production cross-sections, as represented with the three different colours. This result is obtained after a dedicated numerical scan on the set of parameters  $(C_{GG}, C_{BB}, \lambda_\Phi, m_\chi, m_a)$  over the following ranges, keeping  $m_s$  fixed at 750 GeV:

$$\begin{aligned} C_{GG} &\in [5 \times 10^{-4}, 0.1], \quad C_{BB} \in [5 \times 10^{-4}, 0.1], \\ m_\chi &\in [10, 1000] \text{ GeV}, \quad m_a \in [0.2, 2] \text{ GeV}, \\ \lambda_\Phi &\in [0.25, 4]. \end{aligned} \quad (4.10)$$

Finally, we kept only the points respecting

$$1 \text{ fb} \lesssim \sigma_{4\gamma} \lesssim 10 \text{ fb}, \quad 4 \text{ GeV} \lesssim \Gamma_s \lesssim 60 \text{ GeV}, \quad \Omega h^2 \approx 0.12, \quad (4.11)$$

and remain compatible with the relevant accelerator constraints (8 TeV searches of the di-jets,  $Z\gamma$ ,  $ZZ$ , decay length of the pseudoscalar  $\lesssim 1$  meter etc.) as well as with the dark matter detection limits discussed in the previous sub-section. We can clearly distinguish three regions in figure 11: (i) The low mass region ( $m_\chi \lesssim 300$  GeV) in which the relic abundance

<sup>13</sup>A wide gamma-ray box is actually achieved only when  $m_\chi > 400$  GeV. The gamma-ray box is narrow when close to the kinematical threshold and becomes sensitive to the gamma-ray line searches. We have included the corresponding constraint in the parameter scan described in the sub-section 4.4.

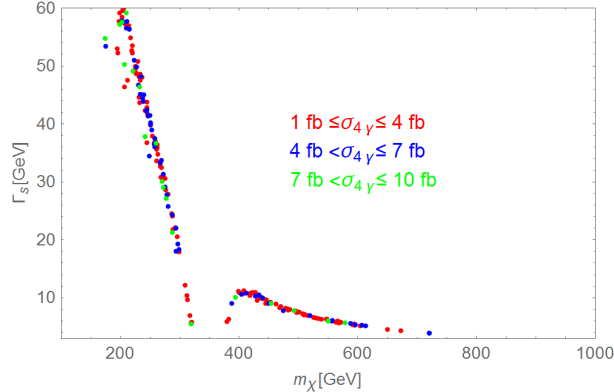


**Figure 11.** Summary plot representing points in the  $(m_\chi, \Gamma_s)$  plane that simultaneously respect the LHC and cosmological constraints and correspond to different di-photon production cross-sections, as depicted with the three different colours.

is dominated by the p-wave (velocity suppressed) annihilation channel  $\bar{\chi}\chi \rightarrow s \rightarrow aa$  (see figure 5). In this case a large width ( $\Gamma_s \gtrsim 20$  GeV) is necessary to compensate the velocity suppression effect and to avoid *overabundance* of the dark matter in the Universe. (ii) In the second region,  $300 \text{ GeV} \lesssim m_\chi \lesssim 400 \text{ GeV}$ , the correct abundance is obtained through the pole region of the same diagram (figure 5). In this case, a narrow width of  $s$  ( $\lesssim 12$  GeV) is necessary to avoid *underabundance* of the dark matter. (iii) Finally, in the last region ( $m_\chi \gtrsim 400 \text{ GeV}$ ), the t-channel (s-wave) annihilation depicted in figure 7 determines the relic abundance of  $\chi$ . As the final state  $sa$  has an odd parity, there is no velocity suppression and a moderate width ( $\sim \mathcal{O}(10 \text{ GeV})$ ) is needed to respect the WMAP/PLANCK constraint.

It is also interesting to notice from figure 11 that if the future ATLAS/CMS analysis determines the value of the width  $\Gamma_s$  more precisely, it will become possible to estimate the dark matter mass, consistent with the cosmological constraint. If the large width scenario is confirmed, an electroweak scale mass will be favoured.

Before moving to the conclusion we just briefly comment on some theoretical aspects relative to our scenario. Our work is motivated by pure phenomenological purposes and thus, we have not referred to any particular setup for the origin of the couplings  $C_{GG}$  and  $C_{BB}$ . As pointed out, for example, in refs. [20, 25, 182, 219, 220], the extra matter needed at the loop level to generate the  $C_{GG}, C_{BB}$  couplings affects the running of the gauge couplings, driving them towards the non-perturbative regime already at energy scales of a few TeV. Thus, too much high values of these couplings remain disfavoured. Similar to ref. [182], we then remark that the low values of the  $C_{GG}, C_{BB}$  couplings needed to fit the observed LHC excess, compared to the case of a resonance decaying into two isolated photons, relax also the theoretical constraints, besides the experimental ones. In scenarios like the one considered in this work, a strong impact is still retained by the renormalization group equation running of the quartic coupling  $\lambda_\Phi$ . In view of this, the higher values of  $\lambda_\Phi$  considered here, corresponding to  $\Gamma_s \sim 40 - 60$  GeV, might result in tension with constraints from the theoretical consistency. On the other hand, we remark that except for  $m_\chi \lesssim 300$  GeV, the phenomenological constraints favour values of  $\Gamma_s$  below 12 GeV. The latter corresponds to  $\lambda_\Phi \lesssim 0.8$  which allows to maintain a safe theoretical framework at least up to an energy scale relevant for the phenomenological analysis.

## 5 Conclusion

We have considered in this note the possibility that the di-photon signal is in reality produced through the decay of two light pseudoscalars into two pairs of highly collimated photons, indistinguishable from the isolated photons. We have shown that, in a spontaneous symmetry breaking framework, once one couples the scalar sector to the dark matter, it appears feasible to re-open a large range of the dark matter masses compatible with all the present experimental constraints.

## Acknowledgments

Y.M. wants to thank especially J.B de Vivie whose help was fundamental throughout our work. The authors thanks Emilian Dudas and Ulrich Ellwanger for fruitful discussions. This work is also supported by the Spanish MICINN's Consolider-Ingenio 2010 Programme under grant Multi-Dark **CSD2009-00064**, the contract **FPA2010-17747**, the France-US PICS no. 06482 and the LIA-TCAP of CNRS. Y. M. and G. A. acknowledges partial support from the European Union FP7 ITN INVISIBLES (Marie Curie Actions, **PITN-GA-2011- 289442**) and the ERC advanced grants Higgs@LHC and MassTeV. G. A. thanks the CERN theory division for the hospitality during part of the completion of this project. P.G. acknowledges the support from P2IO Excellence Laboratory (LABEX). This research was also supported in part by the Research Executive Agency (REA) of the European Union under the Grant Agreement **PITN-GA2012-316704** ("HiggsTools").

## References

- [1] ATLAS collaboration, *Search for resonances decaying to photon pairs in  $3.2 \text{ fb}^{-1}$  of  $pp$  collisions at  $\sqrt{s} = 13 \text{ TeV}$  with the ATLAS detector*, *ATLAS-CONF-2015-081* (2015) .
- [2] CMS collaboration, *Search for new physics in high mass diphoton events in proton-proton collisions at  $13\text{TeV}$* , *CMS-PAS-EXO-15-004* (2015) .
- [3] CMS collaboration, *Search for new physics in high mass diphoton events in  $3.3 \text{ fb}^{-1}$  of proton-proton collisions at  $\sqrt{s} = 13 \text{ TeV}$  and combined interpretation of searches at  $8 \text{ TeV}$  and  $13 \text{ TeV}$* , *CMS-PAS-EXO-16-018* (2016) .
- [4] ATLAS collaboration, *Search for resonances in diphoton events with the ATLAS detector at  $\sqrt{s} = 13 \text{ TeV}$* , *ATLAS-CONF-2016-018* (2016) .
- [5] D. T. Huong and P. V. Dong, *Left-right asymmetry and  $750 \text{ GeV}$  diphoton excess*, *Phys. Rev. D* **93** (2016) 095019, [[1603.05146](#)].
- [6] V. De Romeri, J. S. Kim, V. Martín-Lozano, K. Rolbiecki and R. R. de Austri, *Confronting dark matter with the diphoton excess from a parent resonance decay*, *Eur. Phys. J. C* **76** (2016) 262, [[1603.04479](#)].
- [7] A. Ahriche, G. Faisel, S. Nasri and J. Tandean, *Addressing the LHC  $750 \text{ GeV}$  diphoton excess without new colored states*, [1603.01606](#).
- [8] Y. Tsai, L.-T. Wang and Y. Zhao, *Faking The Diphoton Excess by Displaced Dark Photon Decays*, [1603.00024](#).
- [9] T. Li, J. A. Maxin, V. E. Mayes and D. V. Nanopoulos, *The  $750 \text{ GeV}$  Diphoton Excesses in a Realistic  $D$ -brane Model*, [1602.09099](#).
- [10] G. Lazarides and Q. Shafi, *Diphoton resonances in a  $U(1)_{B-L}$  extension of the minimal supersymmetric standard model*, *Phys. Rev. D* **93** (2016) 111702, [[1602.07866](#)].

- [11] J. Ren and J.-H. Yu, *SU(2) × SU(2) × U(1) Interpretation on the 750 GeV Diphoton Excess*, [1602.07708](#).
- [12] E. Molinaro, F. Sannino and N. Vignaroli, *Collider Tests of (Composite) Diphoton Resonances*, [1602.07574](#).
- [13] M. Redi, A. Strumia, A. Tesi and E. Vigiani, *Di-photon resonance and Dark Matter as heavy pions*, *JHEP* **05** (2016) 078, [[1602.07297](#)].
- [14] P. Ko, T. Nomura, H. Okada and Y. Orikasa, *Confronting a New Three-loop Seesaw Model with the 750 GeV Diphoton Excess*, [1602.07214](#).
- [15] S. Baek and J.-h. Park, *LHC 750 GeV diphoton excess and muon (g − 2)*, *Phys. Lett.* **B758** (2016) 416–422, [[1602.05588](#)].
- [16] F. Staub et al., *Precision tools and models to narrow in on the 750 GeV diphoton resonance*, [1602.05581](#).
- [17] S. F. Mantilla, R. Martinez, F. Ochoa and C. F. Sierra, *Diphoton decay for a 750 GeV scalar boson in a SU(6) ⊗ U(1)<sub>X</sub> model*, [1602.05216](#).
- [18] Y. Hamada, H. Kawai, K. Kawana and K. Tsumura, *Models of LHC Diphoton Excesses Valid up to the Planck scale*, [1602.04170](#).
- [19] C. Gross, O. Lebedev and J. M. No, *Drell-Yan Constraints on New Electroweak States and the Di-photon Anomaly*, [1602.03877](#).
- [20] K. J. Bae, M. Endo, K. Hamaguchi and T. Moroi, *Diphoton Excess and Running Couplings*, *Phys. Lett.* **B757** (2016) 493–500, [[1602.03653](#)].
- [21] S.-F. Ge, H.-J. He, J. Ren and Z.-Z. Xianyu, *Realizing Dark Matter and Higgs Inflation in Light of LHC Diphoton Excess*, *Phys. Lett.* **B757** (2016) 480–492, [[1602.01801](#)].
- [22] T. Li, J. A. Maxin, V. E. Mayes and D. V. Nanopoulos, *A Flippon Related Singlet at the LHC II*, [1602.01377](#).
- [23] R. Ding, Y. Fan, L. Huang, C. Li, T. Li, S. Raza et al., *Systematic Study of Diphoton Resonance at 750 GeV from Sgoldstino*, [1602.00977](#).
- [24] A. Hektor and L. Marzola, *Di-photon excess at LHC and the gamma ray excess at the Galactic Centre*, [1602.00004](#).
- [25] E. Bertuzzo, P. A. N. Machado and M. Taoso, *Di-Photon excess in the 2HDM: hastening towards the instability and the non-perturbative regime*, [1601.07508](#).
- [26] J. Kawamura and Y. Omura, *Diphoton excess at 750 GeV and LHC constraints in models with vectorlike particles*, *Phys. Rev.* **D93** (2016) 115011, [[1601.07396](#)].
- [27] C.-Q. Geng and D. Huang, *Note on Spin-2 Particle Interpretation of the 750 GeV Diphoton Excess*, *Phys. Rev.* **D93** (2016) 115032, [[1601.07385](#)].
- [28] T. Nomura and H. Okada, *Generalized Zee-Babu model with 750 GeV diphoton resonance*, *Phys. Lett.* **B756** (2016) 295–302, [[1601.07339](#)].
- [29] S. F. King and R. Nevzorov, *750 GeV Diphoton Resonance from Singlets in an Exceptional Supersymmetric Standard Model*, *JHEP* **03** (2016) 139, [[1601.07242](#)].
- [30] S. Abel and V. V. Khoze, *Photo-production of a 750 GeV di-photon resonance mediated by Kaluza-Klein leptons in the loop*, *JHEP* **05** (2016) 063, [[1601.07167](#)].
- [31] U. Aydemir and T. Mandal, *Interpretation of the 750 GeV diphoton excess with colored scalars in SO(10) grand unification*, [1601.06761](#).
- [32] C.-W. Chiang and A.-L. Kuo, *Can the 750-GeV diphoton resonance be the singlet Higgs boson of custodial Higgs triplet model?*, [1601.06394](#).

- [33] Q.-H. Cao, Y.-Q. Gong, X. Wang, B. Yan and L. L. Yang, *One bump or two peaks: The 750 GeV diphoton excess and dark matter with a complex mediator*, *Phys. Rev.* **D93** (2016) 075034, [[1601.06374](#)].
- [34] X.-F. Han, L. Wang and J. M. Yang, *An extension of two-Higgs-doublet model and the excesses of 750 GeV diphoton, muon  $g-2$  and  $h \rightarrow \mu\tau$* , *Phys. Lett.* **B757** (2016) 537–547, [[1601.04954](#)].
- [35] W. Chao, *The Diphoton Excess Inspired Electroweak Baryogenesis*, [1601.04678](#).
- [36] T. Nomura and H. Okada, *Four-loop Radiative Seesaw Model with 750 GeV Diphoton Resonance*, [1601.04516](#).
- [37] J. H. Davis, M. Fairbairn, J. Heal and P. Tunney, *The Significance of the 750 GeV Fluctuation in the ATLAS Run 2 Diphoton Data*, [1601.03153](#).
- [38] R. Ding, Z.-L. Han, Y. Liao and X.-D. Ma, *Interpretation of 750 GeV Diphoton Excess at LHC in Singlet Extension of Color-octet Neutrino Mass Model*, *Eur. Phys. J.* **C76** (2016) 204, [[1601.02714](#)].
- [39] J.-H. Yu, *Hidden Gauged  $U(1)$  Model: Unifying Scotogenic Neutrino and Flavor Dark Matter*, *Phys. Rev.* **D93** (2016) 113007, [[1601.02609](#)].
- [40] J. Cao, L. Shang, W. Su, Y. Zhang and J. Zhu, *Interpreting the 750 GeV diphoton excess in the Minimal Dilaton Model*, *Eur. Phys. J.* **C76** (2016) 239, [[1601.02570](#)].
- [41] P. Ko and T. Nomura, *Dark sector shining through 750 GeV dark Higgs boson at the LHC*, *Phys. Lett.* **B758** (2016) 205–211, [[1601.02490](#)].
- [42] C. Hati, *Explaining the diphoton excess in Alternative Left-Right Symmetric Model*, *Phys. Rev.* **D93** (2016) 075002, [[1601.02457](#)].
- [43] D. Stolarski and R. Vega-Morales, *Probing a Virtual Diphoton Excess*, *Phys. Rev.* **D93** (2016) 055008, [[1601.02004](#)].
- [44] D. Borah, S. Patra and S. Sahoo, *Subdominant Left-Right Scalar Dark Matter as Origin of the 750 GeV Di-photon Excess at LHC*, [1601.01828](#).
- [45] S. Fichet, G. von Gersdorff and C. Royon, *Measuring the Diphoton Coupling of a 750 GeV Resonance*, *Phys. Rev. Lett.* **116** (2016) 231801, [[1601.01712](#)].
- [46] I. Sahin, *Semi-elastic cross section for a scalar resonance of mass 750 GeV*, [1601.01676](#).
- [47] F. D’Eramo, J. de Vries and P. Panci, *A 750 GeV Portal: LHC Phenomenology and Dark Matter Candidates*, *JHEP* **05** (2016) 089, [[1601.01571](#)].
- [48] S. Bhattacharya, S. Patra, N. Sahoo and N. Sahu, *750 GeV diphoton excess at CERN LHC from a dark sector assisted scalar decay*, *JCAP* **1606** (2016) 010, [[1601.01569](#)].
- [49] H. Zhang, *The 750GeV Diphoton Excess: Who Introduces It?*, [1601.01355](#).
- [50] H. Ito, T. Moroi and Y. Takaesu, *Studying 750 GeV di-photon resonance at photon-photon collider*, *Phys. Lett.* **B756** (2016) 147–152, [[1601.01144](#)].
- [51] F. F. Deppisch, C. Hati, S. Patra, P. Pritimita and U. Sarkar, *Implications of the diphoton excess on left–right models and gauge unification*, *Phys. Lett.* **B757** (2016) 223–230, [[1601.00952](#)].
- [52] B. Dutta, Y. Gao, T. Ghosh, I. Gogoladze, T. Li, Q. Shafi et al., *Diphoton Excess in Consistent Supersymmetric  $SU(5)$  Models with Vector-like Particles*, [1601.00866](#).
- [53] A. E. C. Hernández, I. d. M. Varzielas and E. Schumacher, *The 750 GeV diphoton resonance in the light of a 2HDM with  $S_3$  flavour symmetry*, [1601.00661](#).
- [54] A. Karozas, S. F. King, G. K. Leontaris and A. K. Meadowcroft, *750 GeV diphoton excess from  $E_6$  in  $F$ -theory GUTs*, *Phys. Lett.* **B757** (2016) 73–78, [[1601.00640](#)].



- [55] W. Chao, *The Diphoton Excess from an Exceptional Supersymmetric Standard Model*, [1601.00633](#).
- [56] U. Danielsson, R. Enberg, G. Ingelman and T. Mandal, *The force awakens - the 750 GeV diphoton excess at the LHC from a varying electromagnetic coupling*, [1601.00624](#).
- [57] K. Ghorbani and H. Ghorbani, *The 750 GeV Diphoton Excess from a Pseudoscalar in Fermionic Dark Matter Scenario*, [1601.00602](#).
- [58] P. Ko, Y. Omura and C. Yu, *Diphoton Excess at 750 GeV in leptophobic  $U(1)'$  model inspired by  $E_6$  GUT*, *JHEP* **04** (2016) 098, [[1601.00586](#)].
- [59] X.-F. Han, L. Wang, L. Wu, J. M. Yang and M. Zhang, *Explaining 750 GeV diphoton excess from top/bottom partner cascade decay in two-Higgs-doublet model extension*, *Phys. Lett. B* **756** (2016) 309–316, [[1601.00534](#)].
- [60] T. Nomura and H. Okada, *Four-loop Neutrino Model Inspired by Diphoton Excess at 750 GeV*, *Phys. Lett. B* **755** (2016) 306–311, [[1601.00386](#)].
- [61] E. Palti, *Vector-Like Exotics in F-Theory and 750 GeV Diphotons*, *Nucl. Phys. B* **907** (2016) 597–616, [[1601.00285](#)].
- [62] A. Dasgupta, M. Mitra and D. Borah, *Minimal Left-Right Symmetry Confronted with the 750 GeV Di-photon Excess at LHC*, [1512.09202](#).
- [63] K. Kaneta, S. Kang and H.-S. Lee, *Diphoton excess at the LHC Run 2 and its implications for a new heavy gauge boson*, [1512.09129](#).
- [64] Y. Jiang, Y.-Y. Li and T. Liu, *750 GeV Resonance in the Gauged  $U(1)'$ -Extended MSSM*, *Phys. Lett. B* **759** (2016) 354–360, [[1512.09127](#)].
- [65] A. E. C. Hernández, *The 750 GeV diphoton resonance can cause the SM fermion mass and mixing pattern*, [1512.09092](#).
- [66] S. Kanemura, N. Machida, S. Odori and T. Shindou, *Diphoton excess at 750 GeV in an extended scalar sector*, [1512.09053](#).
- [67] S. Kanemura, K. Nishiwaki, H. Okada, Y. Orikasa, S. C. Park and R. Watanabe, *LHC 750 GeV Diphoton excess in a radiative seesaw model*, [1512.09048](#).
- [68] X.-J. Huang, W.-H. Zhang and Y.-F. Zhou, *A 750 GeV dark matter messenger at the Galactic Center*, *Phys. Rev. D* **93** (2016) 115006, [[1512.08992](#)].
- [69] Y. Hamada, T. Noumi, S. Sun and G. Shiu, *An  $O(750)$  GeV Resonance and Inflation*, *Phys. Rev. D* **93** (2016) 123514, [[1512.08984](#)].
- [70] S. K. Kang and J. Song, *Top-phobic heavy Higgs boson as the 750 GeV diphoton resonance*, *Phys. Rev. D* **93** (2016) 115012, [[1512.08963](#)].
- [71] L. E. Ibáñez and V. Martín-Lozano, *A Megaxion at 750 GeV as a First Hint of Low Scale String Theory*, [1512.08777](#).
- [72] N. Bizot, S. Davidson, M. Frigerio and J. L. Kneur, *Two Higgs doublets to explain the excesses  $pp \rightarrow \gamma\gamma(750 \text{ GeV})$  and  $h \rightarrow \tau^\pm\mu^\mp$* , *JHEP* **03** (2016) 073, [[1512.08508](#)].
- [73] P. S. B. Dev, R. N. Mohapatra and Y. Zhang, *Quark Seesaw, Vectorlike Fermions and Diphoton Excess*, *JHEP* **02** (2016) 186, [[1512.08507](#)].
- [74] F. Goertz, J. F. Kamenik, A. Katz and M. Nardecchia, *Indirect Constraints on the Scalar Di-Photon Resonance at the LHC*, *JHEP* **05** (2016) 187, [[1512.08500](#)].
- [75] W. Chao, *Neutrino Catalyzed Diphoton Excess*, [1512.08484](#).
- [76] J. Gao, H. Zhang and H. X. Zhu, *Diphoton excess at 750 GeV: gluon-gluon fusion or quark-antiquark annihilation?*, [1512.08478](#).



- [77] J. E. Kim, *Is an axizilla possible for di-photon resonance?*, *Phys. Lett.* **B755** (2016) 190–195, [[1512.08467](#)].
- [78] Q.-H. Cao, Y. Liu, K.-P. Xie, B. Yan and D.-M. Zhang, *Diphoton excess, low energy theorem, and the 331 model*, *Phys. Rev.* **D93** (2016) 075030, [[1512.08441](#)].
- [79] C. Cai, Z.-H. Yu and H.-H. Zhang, *750 GeV diphoton resonance as a singlet scalar in an extra dimensional model*, *Phys. Rev.* **D93** (2016) 075033, [[1512.08440](#)].
- [80] F. Wang, W. Wang, L. Wu, J. M. Yang and M. Zhang, *Interpreting 750 GeV Diphoton Resonance in the NMSSM with Vector-like Particles*, [[1512.08434](#)].
- [81] J. Cao, L. Shang, W. Su, F. Wang and Y. Zhang, *Interpreting The 750 GeV Diphoton Excess Within Topflavor Seesaw Model*, [[1512.08392](#)].
- [82] H. An, C. Cheung and Y. Zhang, *Broad Diphotons from Narrow States*, [[1512.08378](#)].
- [83] Y.-L. Tang and S.-h. Zhu, *NMSSM extended with vector-like particles and the diphoton excess on the LHC*, [[1512.08323](#)].
- [84] G. Li, Y.-n. Mao, Y.-L. Tang, C. Zhang, Y. Zhou and S.-h. Zhu, *Pseudoscalar Decaying Only via Loops as an Explanation for the 750 GeV Diphoton Excess*, *Phys. Rev. Lett.* **116** (2016) 151803, [[1512.08255](#)].
- [85] A. Salvio and A. Mazumdar, *Higgs Stability and the 750 GeV Diphoton Excess*, *Phys. Lett.* **B755** (2016) 469–474, [[1512.08184](#)].
- [86] J.-C. Park and S. C. Park, *Indirect signature of dark matter with the diphoton resonance at 750 GeV*, [[1512.08117](#)].
- [87] H. Han, S. Wang and S. Zheng, *Dark Matter Theories in the Light of Diphoton Excess*, [[1512.07992](#)].
- [88] L. J. Hall, K. Harigaya and Y. Nomura, *750 GeV Diphotons: Implications for Supersymmetric Unification*, *JHEP* **03** (2016) 017, [[1512.07904](#)].
- [89] J. Zhang and S. Zhou, *Electroweak Vacuum Stability and Diphoton Excess at 750 GeV*, *Chin. Phys.* **C40** (2016) 081001, [[1512.07889](#)].
- [90] J. Liu, X.-P. Wang and W. Xue, *LHC diphoton excess from colorful resonances*, [[1512.07885](#)].
- [91] K. Cheung, P. Ko, J. S. Lee, J. Park and P.-Y. Tseng, *A Higgcision study on the 750 GeV Di-photon Resonance and 125 GeV SM Higgs boson with the Higgs-Singlet Mixing*, [[1512.07853](#)].
- [92] K. Das and S. K. Rai, *750 GeV diphoton excess in a U(1) hidden symmetry model*, *Phys. Rev.* **D93** (2016) 095007, [[1512.07789](#)].
- [93] H. Davoudiasl and C. Zhang, *750 GeV messenger of dark conformal symmetry breaking*, *Phys. Rev.* **D93** (2016) 055006, [[1512.07672](#)].
- [94] B. C. Allanach, P. S. B. Dev, S. A. Renner and K. Sakurai, *750 GeV diphoton excess explained by a resonant sneutrino in R-parity violating supersymmetry*, *Phys. Rev.* **D93** (2016) 115022, [[1512.07645](#)].
- [95] J. Gu and Z. Liu, *Physics implications of the diphoton excess from the perspective of renormalization group flow*, *Phys. Rev.* **D93** (2016) 075006, [[1512.07624](#)].
- [96] M. Cvetič, J. Halverson and P. Langacker, *String Consistency, Heavy Exotics, and the 750 GeV Diphoton Excess at the LHC*, [[1512.07622](#)].
- [97] W. Altmannshofer, J. Galloway, S. Gori, A. L. Kagan, A. Martin and J. Zupan, *750 GeV diphoton excess*, *Phys. Rev.* **D93** (2016) 095015, [[1512.07616](#)].
- [98] Q.-H. Cao, S.-L. Chen and P.-H. Gu, *Strong CP Problem, Neutrino Masses and the 750 GeV Diphoton Resonance*, [[1512.07541](#)].

- [99] S. Chakraborty, A. Chakraborty and S. Raychaudhuri, *Diphoton resonance at 750 GeV in the broken MRSSM*, [1512.07527](#).
- [100] M. Badziak, *Interpreting the 750 GeV diphoton excess in minimal extensions of Two-Higgs-Doublet models*, *Phys. Lett.* **B759** (2016) 464–470, [[1512.07497](#)].
- [101] K. M. Patel and P. Sharma, *Interpreting 750 GeV diphoton excess in SU(5) grand unified theory*, *Phys. Lett.* **B757** (2016) 282–288, [[1512.07468](#)].
- [102] S. Moretti and K. Yagyu, *The 750 GeV diphoton excess and its explanation in 2-Higgs Doublet Models with a real inert scalar multiplet*, *Phys. Rev.* **D93** (2016) 055043, [[1512.07462](#)].
- [103] W.-C. Huang, Y.-L. S. Tsai and T.-C. Yuan, *Gauged Two Higgs Doublet Model confronts the LHC 750 GeV diphoton anomaly*, *Nucl. Phys.* **B909** (2016) 122–134, [[1512.07268](#)].
- [104] P. S. B. Dev and D. Teresi, *Asymmetric Dark Matter in the Sun and the Diphoton Excess at the LHC*, [1512.07243](#).
- [105] J. de Blas, J. Santiago and R. Vega-Morales, *New vector bosons and the diphoton excess*, *Phys. Lett.* **B759** (2016) 247–252, [[1512.07229](#)].
- [106] U. K. Dey, S. Mohanty and G. Tomar, *750 GeV Resonance in the Dark Left-Right Model*, *Phys. Lett.* **B756** (2016) 384–389, [[1512.07212](#)].
- [107] A. E. C. Hernández and I. Nisandzic, *LHC diphoton 750 GeV resonance as an indication of  $SU(3)_c \times SU(3)_L \times U(1)_X$  gauge symmetry*, [1512.07165](#).
- [108] C. W. Murphy, *Vector Leptoquarks and the 750 GeV Diphoton Resonance at the LHC*, *Phys. Lett.* **B757** (2016) 192–198, [[1512.06976](#)].
- [109] S. M. Boucenna, S. Morisi and A. Vicente, *The LHC diphoton resonance from gauge symmetry*, *Phys. Rev.* **D93** (2016) 115008, [[1512.06878](#)].
- [110] M. Bauer and M. Neubert, *Flavor anomalies, the 750 GeV diphoton excess, and a dark matter candidate*, *Phys. Rev.* **D93** (2016) 115030, [[1512.06828](#)].
- [111] J. M. Cline and Z. Liu, *LHC diphotons from electroweakly pair-produced composite pseudoscalars*, [1512.06827](#).
- [112] W. S. Cho, D. Kim, K. Kong, S. H. Lim, K. T. Matchev, J.-C. Park et al., *750 GeV Diphoton Excess May Not Imply a 750 GeV Resonance*, *Phys. Rev. Lett.* **116** (2016) 151805, [[1512.06824](#)].
- [113] L. Berthier, J. M. Cline, W. Shepherd and M. Trott, *Effective interpretations of a diphoton excess*, *JHEP* **04** (2016) 084, [[1512.06799](#)].
- [114] J. S. Kim, K. Rolbiecki and R. Ruiz de Austri, *Model-independent combination of diphoton constraints at 750 GeV*, *Eur. Phys. J.* **C76** (2016) 251, [[1512.06797](#)].
- [115] X.-J. Bi, Q.-F. Xiang, P.-F. Yin and Z.-H. Yu, *The 750 GeV diphoton excess at the LHC and dark matter constraints*, *Nucl. Phys.* **B909** (2016) 43–64, [[1512.06787](#)].
- [116] M. Dhuria and G. Goswami, *Perturbativity, vacuum stability and inflation in the light of 750 GeV diphoton excess*, [1512.06782](#).
- [117] J. J. Heckman, *750 GeV Diphotons from a D3-brane*, *Nucl. Phys.* **B906** (2016) 231–240, [[1512.06773](#)].
- [118] F. P. Huang, C. S. Li, Z. L. Liu and Y. Wang, *750 GeV Diphoton Excess from Cascade Decay*, [1512.06732](#).
- [119] J. Cao, C. Han, L. Shang, W. Su, J. M. Yang and Y. Zhang, *Interpreting the 750 GeV diphoton excess by the singlet extension of the Manohar-Wise model*, *Phys. Lett.* **B755** (2016) 456–463, [[1512.06728](#)].

- [120] F. Wang, L. Wu, J. M. Yang and M. Zhang, *750 GeV diphoton resonance, 125 GeV Higgs and muon  $g - 2$  anomaly in deflected anomaly mediation SUSY breaking scenarios*, *Phys. Lett.* **B759** (2016) 191–199, [[1512.06715](#)].
- [121] T.-F. Feng, X.-Q. Li, H.-B. Zhang and S.-M. Zhao, *The LHC 750 GeV diphoton excess in supersymmetry with gauged baryon and lepton numbers*, [[1512.06696](#)].
- [122] D. Bardhan, D. Bhatia, A. Chakraborty, U. Maitra, S. Raychaudhuri and T. Samui, *Radion Candidate for the LHC Diphoton Resonance*, [[1512.06674](#)].
- [123] J. Chang, K. Cheung and C.-T. Lu, *Interpreting the 750 GeV diphoton resonance using photon jets in hidden-valley-like models*, *Phys. Rev.* **D93** (2016) 075013, [[1512.06671](#)].
- [124] M.-x. Luo, K. Wang, T. Xu, L. Zhang and G. Zhu, *Squarkonium, diquarkonium and octetonium at the LHC and their di-photon decays*, *Phys. Rev.* **D93** (2016) 055042, [[1512.06670](#)].
- [125] X.-F. Han and L. Wang, *Implication of the 750 GeV diphoton resonance on two-Higgs-doublet model and its extensions with Higgs field*, *Phys. Rev.* **D93** (2016) 055027, [[1512.06587](#)].
- [126] H. Han, S. Wang and S. Zheng, *Scalar Explanation of Diphoton Excess at LHC*, *Nucl. Phys.* **B907** (2016) 180–186, [[1512.06562](#)].
- [127] R. Ding, L. Huang, T. Li and B. Zhu, *Interpreting 750 GeV Diphoton Excess with R-parity Violation Supersymmetry*, [[1512.06560](#)].
- [128] I. Chakraborty and A. Kundu, *Diphoton excess at 750 GeV: Singlet scalars confront triviality*, *Phys. Rev.* **D93** (2016) 055003, [[1512.06508](#)].
- [129] S. Chang, *A Simple U(1) Gauge Theory Explanation of the Diphoton Excess*, *Phys. Rev.* **D93** (2016) 055016, [[1512.06426](#)].
- [130] C. Han, H. M. Lee, M. Park and V. Sanz, *The diphoton resonance as a gravity mediator of dark matter*, *Phys. Lett.* **B755** (2016) 371–379, [[1512.06376](#)].
- [131] W. Chao, *Symmetries behind the 750 GeV diphoton excess*, *Phys. Rev.* **D93** (2016) 115013, [[1512.06297](#)].
- [132] J. Bernon and C. Smith, *Could the width of the diphoton anomaly signal a three-body decay?*, *Phys. Lett.* **B757** (2016) 148–153, [[1512.06113](#)].
- [133] L. M. Carpenter, R. Colburn and J. Goodman, *Supersoft SUSY Models and the 750 GeV Diphoton Excess, Beyond Effective Operators*, [[1512.06107](#)].
- [134] A. Alves, A. G. Dias and K. Sinha, *The 750 GeV S-cion: Where else should we look for it?*, *Phys. Lett.* **B757** (2016) 39–46, [[1512.06091](#)].
- [135] J. S. Kim, J. Reuter, K. Rolbiecki and R. Ruiz de Austri, *A resonance without resonance: scrutinizing the diphoton excess at 750 GeV*, *Phys. Lett.* **B755** (2016) 403–408, [[1512.06083](#)].
- [136] R. Benbrik, C.-H. Chen and T. Nomura, *Higgs singlet boson as a diphoton resonance in a vectorlike quark model*, *Phys. Rev.* **D93** (2016) 055034, [[1512.06028](#)].
- [137] E. Gabrielli, K. Kannike, B. Mele, M. Raidal, C. Spethmann and H. Veermäe, *A SUSY Inspired Simplified Model for the 750 GeV Diphoton Excess*, *Phys. Lett.* **B756** (2016) 36–41, [[1512.05961](#)].
- [138] Y. Bai, J. Berger and R. Lu, *750 GeV dark pion: Cousin of a dark G-parity odd WIMP*, *Phys. Rev.* **D93** (2016) 076009, [[1512.05779](#)].
- [139] C. Csáki, J. Hubisz and J. Terning, *Minimal model of a diphoton resonance: Production without gluon couplings*, *Phys. Rev.* **D93** (2016) 035002, [[1512.05776](#)].
- [140] J. Chakraborty, A. Choudhury, P. Ghosh, S. Mondal and T. Srivastava, *Di-photon resonance around 750 GeV: shedding light on the theory underneath*, [[1512.05767](#)].

- [141] L. Bian, N. Chen, D. Liu and J. Shu, *Hidden confining world on the 750 GeV diphoton excess*, *Phys. Rev.* **D93** (2016) 095011, [[1512.05759](#)].
- [142] D. Curtin and C. B. Verhaaren, *Quirky Explanations for the Diphoton Excess*, *Phys. Rev.* **D93** (2016) 055011, [[1512.05753](#)].
- [143] W. Chao, R. Huo and J.-H. Yu, *The Minimal Scalar-Stealth Top Interpretation of the Diphoton Excess*, [1512.05738](#).
- [144] S. V. Demidov and D. S. Gorbunov, *On the sgoldstino interpretation of the diphoton excess*, *JETP Lett.* **103** (2016) 219–222, [[1512.05723](#)].
- [145] J. M. No, V. Sanz and J. Setford, *See-saw composite Higgs model at the LHC: Linking naturalness to the 750 GeV diphoton resonance*, *Phys. Rev.* **D93** (2016) 095010, [[1512.05700](#)].
- [146] D. Bečirević, E. Bertuzzo, O. Sumensari and R. Zukanovich Funchal, *Can the new resonance at LHC be a CP-Odd Higgs boson?*, *Phys. Lett.* **B757** (2016) 261–267, [[1512.05623](#)].
- [147] P. Cox, A. D. Medina, T. S. Ray and A. Spray, *Diphoton Excess at 750 GeV from a Radion in the Bulk-Higgs Scenario*, [1512.05618](#).
- [148] R. Martinez, F. Ochoa and C. F. Sierra, *Diphoton decay for a 750 GeV scalar boson in an  $U(1)'$  model*, [1512.05617](#).
- [149] A. Kobakhidze, F. Wang, L. Wu, J. M. Yang and M. Zhang, *750 GeV diphoton resonance in a top and bottom seesaw model*, *Phys. Lett.* **B757** (2016) 92–96, [[1512.05585](#)].
- [150] Q.-H. Cao, Y. Liu, K.-P. Xie, B. Yan and D.-M. Zhang, *A Boost Test of Anomalous Diphoton Resonance at the LHC*, [1512.05542](#).
- [151] E. Molinaro, F. Sannino and N. Vignaroli, *Minimal Composite Dynamics versus Axion Origin of the Diphoton excess*, [1512.05334](#).
- [152] C. Petersson and R. Torre, *750 GeV Diphoton Excess from the Goldstino Superpartner*, *Phys. Rev. Lett.* **116** (2016) 151804, [[1512.05333](#)].
- [153] R. S. Gupta, S. Jäger, Y. Kats, G. Perez and E. Stamou, *Interpreting a 750 GeV Diphoton Resonance*, [1512.05332](#).
- [154] B. Bellazzini, R. Franceschini, F. Sala and J. Serra, *Goldstones in Diphotons*, *JHEP* **04** (2016) 072, [[1512.05330](#)].
- [155] T. Higaki, K. S. Jeong, N. Kitajima and F. Takahashi, *The QCD Axion from Aligned Axions and Diphoton Excess*, *Phys. Lett.* **B755** (2016) 13–16, [[1512.05295](#)].
- [156] S. Di Chiara, L. Marzola and M. Raidal, *First interpretation of the 750 GeV diphoton resonance at the LHC*, *Phys. Rev.* **D93** (2016) 095018, [[1512.04939](#)].
- [157] A. Pilaftsis, *Diphoton Signatures from Heavy Axion Decays at the CERN Large Hadron Collider*, *Phys. Rev.* **D93** (2016) 015017, [[1512.04931](#)].
- [158] D. Buttazzo, A. Greljo and D. Marzocca, *Knocking on new physics' door with a scalar resonance*, *Eur. Phys. J.* **C76** (2016) 116, [[1512.04929](#)].
- [159] Y. Nakai, R. Sato and K. Tobioka, *Footprints of New Strong Dynamics via Anomaly and the 750 GeV Diphoton*, *Phys. Rev. Lett.* **116** (2016) 151802, [[1512.04924](#)].
- [160] K. Harigaya and Y. Nomura, *Composite Models for the 750 GeV Diphoton Excess*, *Phys. Lett.* **B754** (2016) 151–156, [[1512.04850](#)].
- [161] A. Bharucha, A. Djouadi and A. Goudelis, *Threshold enhancement of diphoton resonances*, [1603.04464](#).
- [162] A. Djouadi, J. Ellis, R. Godbole and J. Quevillon, *Future Collider Signatures of the Possible 750 GeV State*, *JHEP* **03** (2016) 205, [[1601.03696](#)].

- [163] A. Falkowski, O. Slone and T. Volansky, *Phenomenology of a 750 GeV Singlet*, *JHEP* **02** (2016) 152, [[1512.05777](#)].
- [164] B. Dutta, Y. Gao, T. Ghosh, I. Gogoladze and T. Li, *Interpretation of the diphoton excess at CMS and ATLAS*, *Phys. Rev.* **D93** (2016) 055032, [[1512.05439](#)].
- [165] M. Low, A. Tesi and L.-T. Wang, *A pseudoscalar decaying to photon pairs in the early LHC Run 2 data*, *JHEP* **03** (2016) 108, [[1512.05328](#)].
- [166] J. Ellis, S. A. R. Ellis, J. Quevillon, V. Sanz and T. You, *On the Interpretation of a Possible  $\sim 750$  GeV Particle Decaying into  $\gamma\gamma$* , *JHEP* **03** (2016) 176, [[1512.05327](#)].
- [167] S. D. McDermott, P. Meade and H. Ramani, *Singlet Scalar Resonances and the Diphoton Excess*, *Phys. Lett.* **B755** (2016) 353–357, [[1512.05326](#)].
- [168] A. Angelescu, A. Djouadi and G. Moreau, *Scenarii for interpretations of the LHC diphoton excess: two Higgs doublets and vector-like quarks and leptons*, *Phys. Lett.* **B756** (2016) 126–132, [[1512.04921](#)].
- [169] R. Franceschini, G. F. Giudice, J. F. Kamenik, M. McCullough, A. Pomarol, R. Rattazzi et al., *What is the  $\gamma\gamma$  resonance at 750 GeV?*, *JHEP* **03** (2016) 144, [[1512.04933](#)].
- [170] CMS collaboration, *Search for Resonances Decaying to Dijet Final States at  $\sqrt{s} = 8$  TeV with Scouting Data*, *CMS-PAS-EXO-14-005* (2015) .
- [171] ATLAS collaboration, G. Aad et al., *Search for new phenomena in the dijet mass distribution using  $p - p$  collision data at  $\sqrt{s} = 8$  TeV with the ATLAS detector*, *Phys. Rev.* **D91** (2015) 052007, [[1407.1376](#)].
- [172] S. Fichet, G. von Gersdorff and C. Royon, *Scattering light by light at 750 GeV at the LHC*, *Phys. Rev.* **D93** (2016) 075031, [[1512.05751](#)].
- [173] Y. Mambrini, G. Arcadi and A. Djouadi, *The LHC diphoton resonance and dark matter*, *Phys. Lett.* **B755** (2016) 426–432, [[1512.04913](#)].
- [174] M. Backovic, A. Mariotti and D. Redigolo, *Di-photon excess illuminates Dark Matter*, *JHEP* **03** (2016) 157, [[1512.04917](#)].
- [175] D. Barducci, A. Goudelis, S. Kulkarni and D. Sengupta, *One jet to rule them all: monojet constraints and invisible decays of a 750 GeV diphoton resonance*, *JHEP* **05** (2016) 154, [[1512.06842](#)].
- [176] X. Chu, T. Hambye, T. Scarna and M. H. G. Tytgat, *What if Dark Matter Gamma-Ray Lines come with Gluon Lines?*, *Phys. Rev.* **D86** (2012) 083521, [[1206.2279](#)].
- [177] CMS collaboration, V. Khachatryan et al., *Search for dark matter, extra dimensions, and unparticles in monojet events in proton - proton collisions at  $\sqrt{s} = 8$  TeV*, *Eur. Phys. J.* **C75** (2015) 235, [[1408.3583](#)].
- [178] ATLAS collaboration, G. Aad et al., *Search for pair-produced third-generation squarks decaying via charm quarks or in compressed supersymmetric scenarios in  $pp$  collisions at  $\sqrt{s} = 8$  TeV with the ATLAS detector*, *Phys. Rev.* **D90** (2014) 052008, [[1407.0608](#)].
- [179] B. Dasgupta, J. Kopp and P. Schwaller, *Photons, Photon Jets and Dark Photons at 750 GeV and Beyond*, *Eur. Phys. J.* **C76** (2016) 277, [[1602.04692](#)].
- [180] X.-J. Bi, R. Ding, Y. Fan, L. Huang, C. Li, T. Li et al., *A Promising Interpretation of Diphoton Resonance at 750 GeV*, [[1512.08497](#)].
- [181] S. Knapen, T. Melia, M. Papucci and K. Zurek, *Rays of light from the LHC*, *Phys. Rev.* **D93** (2016) 075020, [[1512.04928](#)].
- [182] L. Aparicio, A. Azatov, E. Hardy and A. Romanino, *Diphotons from Diaxions*, *JHEP* **05** (2016) 077, [[1602.00949](#)].



- [183] M. Badziak, M. Olechowski, S. Pokorski and K. Sakurai, *Interpreting 750 GeV Diphoton Excess in Plain NMSSM*, [1603.02203](#).
- [184] F. Domingo, S. Heinemeyer, J. S. Kim and K. Rolbiecki, *The NMSSM lives: with the 750 GeV diphoton excess*, *Eur. Phys. J.* **C76** (2016) 249, [[1602.07691](#)].
- [185] U. Ellwanger and C. Hugonie, *A 750 GeV Diphoton Signal from a Very Light Pseudoscalar in the NMSSM*, *JHEP* **05** (2016) 114, [[1602.03344](#)].
- [186] B. A. Dobrescu, G. L. Landsberg and K. T. Matchev, *Higgs boson decays to CP odd scalars at the Tevatron and beyond*, *Phys. Rev.* **D63** (2001) 075003, [[hep-ph/0005308](#)].
- [187] B. A. Dobrescu and K. T. Matchev, *Light axion within the next-to-minimal supersymmetric standard model*, *JHEP* **09** (2000) 031, [[hep-ph/0008192](#)].
- [188] WMAP collaboration, G. Hinshaw et al., *Nine-Year Wilkinson Microwave Anisotropy Probe (WMAP) Observations: Cosmological Parameter Results*, *Astrophys. J. Suppl.* **208** (2013) 19, [[1212.5226](#)].
- [189] PLANCK collaboration, P. A. R. Ade et al., *Planck 2013 results. XVI. Cosmological parameters*, *Astron. Astrophys.* **571** (2014) A16, [[1303.5076](#)].
- [190] CMS collaboration, S. Chatrchyan et al., *Energy Calibration and Resolution of the CMS Electromagnetic Calorimeter in pp Collisions at  $\sqrt{s} = 7$  TeV*, *JINST* **8** (2013) P09009, [[1306.2016](#)].
- [191] ATLAS collaboration, *Measurements of the photon identification efficiency with the ATLAS detector using  $4.9 \text{ fb}^{-1}$  of pp collision data collected in 2011*, ATLAS-CONF-2012-123 (2012) .
- [192] P. Agrawal, J. Fan, B. Heidenreich, M. Reece and M. Strassler, *Experimental Considerations Motivated by the Diphoton Excess at the LHC*, *JHEP* **06** (2016) 082, [[1512.05775](#)].
- [193] M. Chala, M. Duerr, F. Kahlhoefer and K. Schmidt-Hoberg, *Tricking Landau-Yang: How to obtain the diphoton excess from a vector resonance*, *Phys. Lett.* **B755** (2016) 145–149, [[1512.06833](#)].
- [194] B. Döbrich, J. Jaeckel, F. Kahlhoefer, A. Ringwald and K. Schmidt-Hoberg, *ALPtraum: ALP production in proton beam dump experiments*, *JHEP* **02** (2016) 018, [[1512.03069](#)].
- [195] CMS collaboration, *Search for scalar resonances in the 200–1200 GeV mass range decaying into a Z and a photon in pp collisions at  $\sqrt{s} = 8$  TeV*, CMS-PAS-HIG-16-014 (2016) .
- [196] ATLAS collaboration, G. Aad et al., *Search for an additional, heavy Higgs boson in the  $H \rightarrow ZZ$  decay channel at  $\sqrt{s} = 8$  TeV in pp collision data with the ATLAS detector*, *Eur. Phys. J.* **C76** (2016) 45, [[1507.05930](#)].
- [197] CMS collaboration, V. Khachatryan et al., *Search for a Higgs Boson in the Mass Range from 145 to 1000 GeV Decaying to a Pair of W or Z Bosons*, *JHEP* **10** (2015) 144, [[1504.00936](#)].
- [198] ATLAS collaboration, G. Aad et al., *Search for new resonances in  $W\gamma$  and  $Z\gamma$  final states in pp collisions at  $\sqrt{s} = 8$  TeV with the ATLAS detector*, *Phys. Lett.* **B738** (2014) 428–447, [[1407.8150](#)].
- [199] CMS collaboration, *Search for scalar resonances in the 200-500 GeV mass range decaying into a Z and a photon in pp collisions at  $\sqrt{s} = 8$  TeV*, CMS-PAS-HIG-14-031 (2015) .
- [200] P. Draper and D. McKeen, *Diphotons from Tetraphotons in the Decay of a 125 GeV Higgs at the LHC*, *Phys. Rev.* **D85** (2012) 115023, [[1204.1061](#)].
- [201] ATLAS collaboration, G. Aad et al., *Search for new phenomena in dijet mass and angular distributions from pp collisions at  $\sqrt{s} = 13$  TeV with the ATLAS detector*, *Phys. Lett.* **B754** (2016) 302–322, [[1512.01530](#)].
- [202] CMS collaboration, V. Khachatryan et al., *Search for narrow resonances decaying to dijets in proton-proton collisions at  $\sqrt{s} = 13$  TeV*, *Phys. Rev. Lett.* **116** (2016) 071801, [[1512.01224](#)].

- [203] A. D. Martin, W. J. Stirling, R. S. Thorne and G. Watt, *Heavy-quark mass dependence in global PDF analyses and 3- and 4-flavour parton distributions*, *Eur. Phys. J.* **C70** (2010) 51–72, [[1007.2624](#)].
- [204] A. D. Martin, W. J. Stirling, R. S. Thorne and G. Watt, *Uncertainties on  $\alpha(S)$  in global PDF analyses and implications for predicted hadronic cross sections*, *Eur. Phys. J.* **C64** (2009) 653–680, [[0905.3531](#)].
- [205] A. D. Martin, W. J. Stirling, R. S. Thorne and G. Watt, *Parton distributions for the LHC*, *Eur. Phys. J.* **C63** (2009) 189–285, [[0901.0002](#)].
- [206] L. A. Harland-Lang, V. A. Khoze and M. G. Ryskin, *The production of a diphoton resonance via photon-photon fusion*, *JHEP* **03** (2016) 182, [[1601.07187](#)].
- [207] FERMI-LAT collaboration, M. Ackermann et al., *Searching for Dark Matter Annihilation from Milky Way Dwarf Spheroidal Galaxies with Six Years of Fermi Large Area Telescope Data*, *Phys. Rev. Lett.* **115** (2015) 231301, [[1503.02641](#)].
- [208] FERMI-LAT collaboration, M. Ackermann et al., *Dark matter constraints from observations of 25 Milky Way satellite galaxies with the Fermi Large Area Telescope*, *Phys. Rev.* **D89** (2014) 042001, [[1310.0828](#)].
- [209] FERMI-LAT collaboration, M. Ackermann et al., *Updated search for spectral lines from Galactic dark matter interactions with pass 8 data from the Fermi Large Area Telescope*, *Phys. Rev.* **D91** (2015) 122002, [[1506.00013](#)].
- [210] G. Bélanger, F. Boudjema, A. Pukhov and A. Semenov, *micrOMEGAs4.1: two dark matter candidates*, *Comput. Phys. Commun.* **192** (2015) 322–329, [[1407.6129](#)].
- [211] P. Gondolo and G. Gelmini, *Cosmic abundances of stable particles: Improved analysis*, *Nucl. Phys.* **B360** (1991) 145–179.
- [212] X. Chu, Y. Mambrini, J. Quevillon and B. Zaldivar, *Thermal and non-thermal production of dark matter via  $Z'$ -portal(s)*, *JCAP* **1401** (2014) 034, [[1306.4677](#)].
- [213] X. Chu, T. Hambye and M. H. G. Tytgat, *The Four Basic Ways of Creating Dark Matter Through a Portal*, *JCAP* **1205** (2012) 034, [[1112.0493](#)].
- [214] L. J. Hall, K. Jedamzik, J. March-Russell and S. M. West, *Freeze-In Production of FIMP Dark Matter*, *JHEP* **03** (2010) 080, [[0911.1120](#)].
- [215] E. Dudas, L. Heurtier and Y. Mambrini, *Generating X-ray lines from annihilating dark matter*, *Phys. Rev.* **D90** (2014) 035002, [[1404.1927](#)].
- [216] LUX collaboration, D. S. Akerib et al., *Improved Limits on Scattering of Weakly Interacting Massive Particles from Reanalysis of 2013 LUX Data*, *Phys. Rev. Lett.* **116** (2016) 161301, [[1512.03506](#)].
- [217] A. Ibarra, H. M. Lee, S. López Gehler, W.-I. Park and M. Pato, *Gamma-ray boxes from axion-mediated dark matter*, *JCAP* **1305** (2013) 016, *1603* (2016) E01, [[1303.6632](#)].
- [218] A. Ibarra, A. S. Lamperstorfer, S. López-Gehler, M. Pato and G. Bertone, *On the sensitivity of CTA to gamma-ray boxes from multi-TeV dark matter*, *JCAP* **1509** (2015) 048, [[1503.06797](#)].
- [219] A. Salvio, F. Staub, A. Strumia and A. Urbano, *On the maximal diphoton width*, *JHEP* **03** (2016) 214, [[1602.01460](#)].
- [220] M. Son and A. Urbano, *A new scalar resonance at 750 GeV: Towards a proof of concept in favor of strongly interacting theories*, *JHEP* **05** (2016) 181, [[1512.08307](#)].